DYNAMICS OF MICROBIAL GROWTH IN SINGLE SUBSTRATE CULTURE

By

JASON NOEL

A DISSERTATION PRESENTED TO THE GRADUATE SCHOOL
OF THE UNIVERSITY OF FLORIDA IN PARTIAL FULFILLMENT
OF THE REQUIREMENTS FOR THE DEGREE OF
DOCTOR OF PHILOSOPHY

UNIVERSITY OF FLORIDA

2007

To my Parents David and Tracey Noel

ACKNOWLEDGMENTS

I would first like to acknowledge my advisor Dr. Atul Narang for his guidance and support during this research. Without his ideas and insight none of this would have been possible. I would also like to thank my committee members Dr. Spyros Svoronos, Dr. Ben Koopman, Dr. Ranganathan Narayanan, and Dr. Lewis Johns for their support.

I would also like to thank some individuals whose technical expertise and personal assistance made this research possible. Dr. Thomas Egli from the Swiss Federal Institute of Aquatic Science and Technology was extremely helpful in troubleshooting problems found in operating a chemostat growing microbial cells. Dr. Tommaso Cataldi from the Universita degli Studi della Basisilicate was instrumental in developing a reliable procedure for HPLC quantification of low sugar concentrations in samples extracted from bacterial cultures. Lastly I would like to thank Dr. Max Teplitski from the University of Florida for his help providing a reliable mechanical disruption technique for starved bacteria.

I would like to thank my lab members Dr. Shaki Gupta, Dr. Eric May, Dr. Karthik Subramanian, Ved Sharma, and Brenton Cox. Your technical support and companionship helped make the sometimes frustrating experimental work tolerable. Lastly I would like to thank my friends and family for being there for me through the good times and the bad.

TABLE OF CONTENTS

page

LIST OF TABLES

LIST OF FIGURES

Abstract of Dissertation Presented to the Graduate School
of the University of Florida in Partial Fulfillment of the
Requirements for the Degree of Doctor of Philosophy

DYNAMICS OF MICROBIAL GROWTH IN SINGLE SUBSTRATE CULTURE

By

Jason Noel

August 2007

Chair: Spyros A. Svoronos
Major: Chemical Engineering

In this study the results of continuous to batch mode experiments conducted to characterize the initial transient response of carbon limited microbial cells growing in a chemostat to a pulse of the growth limiting substrate are presented. Changes in cellular rates of growth, substrate uptake, carbon dioxide evolution, and organic carbon excretion were recorded for three different preculture conditions. To ensure the validity of the data, ninety percent of added carbon was accounted for in generated biomass, evolved carbon dioxide, and in excreted organic products before and after the substrate pulse.

The continuous shifts revealed that values of growth and respiration were proportional to the preculture dilution rate while the capacity to increase the respiration and growth rate was inversely proportional to the preculture dilution rate. Saturation of respiration and biosynthetic capacity led to a high amount of excretion at the intermediate and highest preculture dilution rates tested. Only the highest preculture dilution rate was able to utilize the excreted carbon before the specific carbon dioxide evolution rate fell considerably due to lack of substrate.

The identity of the biosynthetic growth limitation was also explored in this study using similar continuous to batch shift experiments. Evidence was found to support the hypothesis that the biosynthetic limitation is an amino acid supply limitation and not a protein production

capacity limitation. Continuous to batch mode shifts followed by a pulse of growth limiting carbon substrate show the transient response of the biosynthetic enzyme glutamate dehydrogenase qualitatively matched the transient response of the intracellular RNA concentration suggesting the enzyme was more likely to be the cause of the biosynthetic growth limitation rather than the intracellular ribosome concentration.

CHAPTER 1
GENERAL INTRODUCTION

1.1 Motivation for Research

The chemostat is the best laboratory approximation to natural water bodies and industrial bioreactors. Naturally the transient response of a chemostat is a problem of significant biological and engineering interest. The simplest dynamics are obtained when a single microbial species is grown on a single growth limiting substrate. The dynamics are complex despite the simplicity of the system. The complexity arises from the ability of cells to adapt to changes in the environment around them. Certain intracellular components adapt to this change on a slow time scale of hours and even days. An example of the effects of this slow adaptation to environmental change can be seen in Figure 1-1.

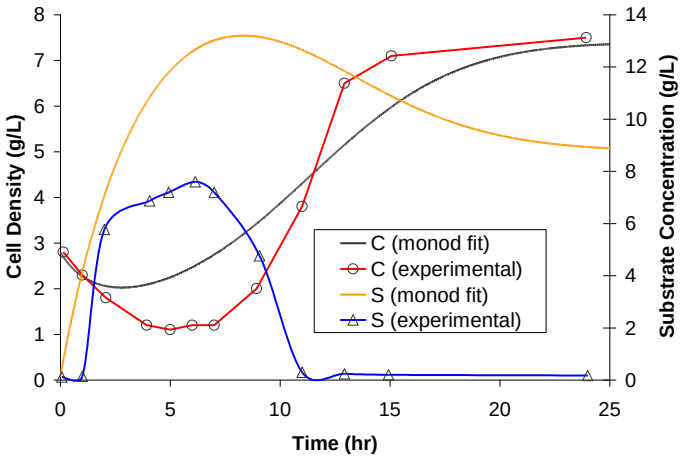

Figure 1-1. Dilution rate shift up from D=0.004 to 0.240 hr^{-1} of continuously grown *K. aerogenes*. [Reprinted without permission. **Phipps, D. W. T. a. P. J.** 1967. Studies on the growth of Aerobacter aerogenes at low dilution rates in a chemostat. Microbial Physiology and Continuous Culture. Her Majesty's Stationary Office**:**240-253. (Pages 360, Figure 2).] A least squares Monod Model (including death rate) fit of the cell density data and substrate concentration has been added. The error in the predicted cell density and actual cell density was minimized with non-zero parameter value constraints and a upper limit of 0.8 for the yield. The Monod Model predicts the decrease in cell density but does so with unrealistic parameters values and a large amount of error in the reactor substrate concentration. Clearly better models are needed to predict these kinds of transients.

Upon an increase in the flow rate of feed in to the chemostat there is a pronounced transient decrease in the cell density and increase in the glucose concentration that ends fifteen hours after the dilution rate shift up. Transients such as these can lead to product deterioration in industrial bioreactors and regulatory violations in waste water treatment facilities as such systems can be disturbed with perturbations to their feed flow rate. As seen in Figure 1-1 the estimated cell density time evolution based on the well known Monod Model does a poor job of predicting the transient response in microbial cells associated with an increase in the feed flow rate in to the chemostat. Better model based control of such systems would be necessary to lessen the impact of such transients in industrial systems.

Based on a review of the experimental literature, conducted by Dr. Atul Narang, two slow variables were hypothesized to control the dynamics of the chemostat: transport enzyme levels and biosynthetic capacity. Under certain operating conditions, the dynamics of the chemostat are controlled by only one of these slow variables. The goals of this research were two fold. The first was to characterize how microbial cells grown at a range of carbon limited growth rates respond to environmental conditions brought about by a feed rate increase perturbation. The second goal was to identify the intracellular cause of this biosynthetic limitation.

1.2 Conceptual Model of the Cell

Figure 1-2 is the conceptual model of growth used to design the experiments completed in this work. The dashed line corresponds to the boundary between the external and internal environments of a cell. Carbonaceous substrate, denoted **S**, enters the cell through transport enzymes, denoted **E**. Typically microbial cells will modify sequestered substrate to an internalized form denoted by **X**. There is possible positive feedback as internalized substrate can induce the synthesis of more of the transport enzyme responsible for the uptake of the substrate as seen with the lac operon. The internalized substrate is converted to a pool of precursor

catabolites denoted by **P**. There is negative feedback inhibition possible here as precursor catabolite excess could inhibit the uptake of more substrate. The precursor catabolites typically have three possible fates. These products of substrate catabolism can be either channeled into additional cell mass, fully oxidized to carbon dioxide, or excreted as a partially catabolized organic molecule. Storage of internalized carbohydrates such as glycogen is denoted by **Ps** and excretion of partially catabolized substrate is denoted by **Px**. Synthesis of protein is denoted by **C-**. The designations **GDH**, **aa, and RNA** stand for glutamate dehydrogenase, amino acids, and RNA, respectively.

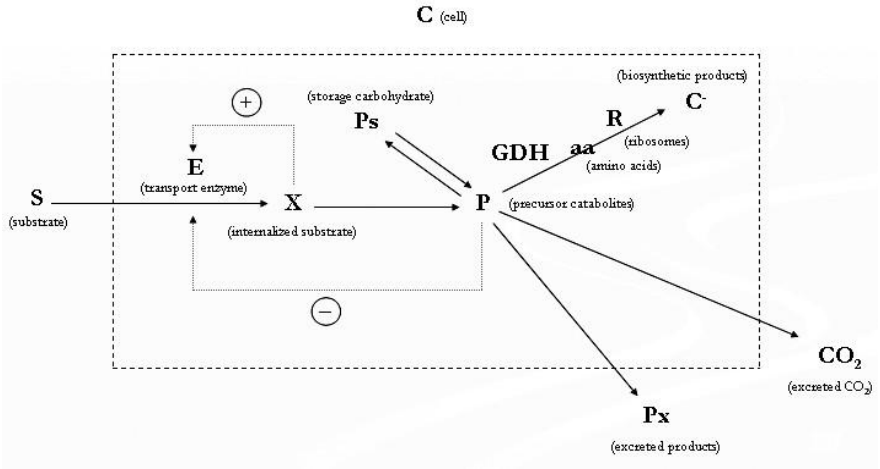

Figure 1-2. Conceptual model of a microbial cell.

1.3 Steady state behavior of microbial cells

For a given microbial species, growth limiting substrate, media composition, pH and temperature the steady states of a chemostat depend on two parameters: the substrate feed concentration and the residual substrate concentration of the reactor bulk. If the substrate feed concentration is increased at a fixed dilution rate, there is no change in the steady state substrate concentration. An increase in the feed concentration is compensated by a proportional increase in the cell density (41). Since the cellular steady state is completely determined by the state of the environment, the steady state values of the cellular variables must also be independent of the

feed concentration. Variation of the steady states with respect to the dilution rate produces more complex results. Located in Figure 1-3, Figure 1-4, Figure 1-5, Figure 1-6, and Figure 1-7 are experimental data from the literature illustrating the dilution rate dependence of some common cellular variables in a carbon limited chemostat.

1.4 Cell density and Substrate Concentration

Cells wash out at both small and large dilution rates. The lower washout dilution rate, called the minimum growth rate, has been argued to be caused by the specific uptake of glucose not being able to meet the minimum maintenance requirement of the cells. Tempest et al. found steady states of glycerol-limited cultures of *K. aerogenes* at dilution rates as low as 0.004 hr^{-1}, and found that the specific growth rate of the viable cells approached a minimum value of 0.009 hr^{-1} (33).

The cell density passes through a maximum between the two washout dilution rates and since the steady state substrate concentration equals the substrate feed concentration at dilution rates above and below the two washout dilution rates the substrate concentration would pass through a minimum value. The data from Figure 1-4 shows the substrate concentration appears as an increasing function of the dilution rate.

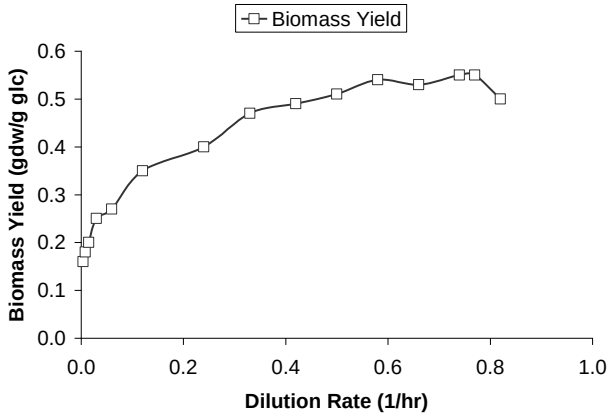

Figure 1-3. Example of dilution rate dependence of biomass yield of microorganisms. The biomass yield data was from *K. aerogenes* grown on minimal media. [Reprinted without permission. **Phipps, D. W. T. a. P. J.** 1967. Studies on the growth of Aerobacter aerogenes at low dilution rates in a chemostat. Microbial Physiology and Continuous Culture. Her Majesty's Stationary Office**:**240-253.1965 (Pages 361, Figure 3), Microbiological Research Establishment, Porton, Salisbury, Wilks, UK.]

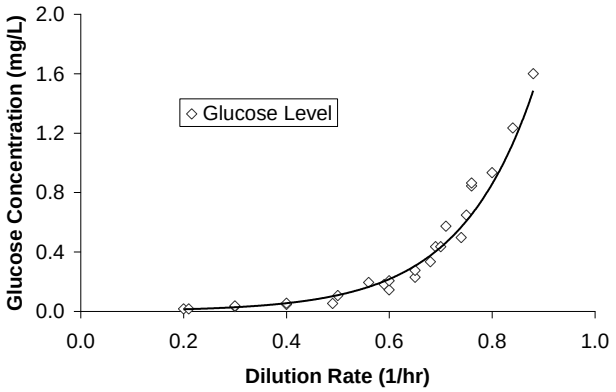

Figure 1-4. Example of dilution rate dependence of the steady state glucose concentration. The glucose data was from *E. coli* ML308 grown on minimal media. [Reprinted without permission. **Senn, H., U. Lendenmann, M. Snozzi, G. Hamer, and T. Egli.** 1994. The growth of Escherichia coli in glucose-limited chemostat cultures: a re-examination of the kinetics. Biochim Biophys Acta **1201:**424-36. (Page 428, Table 2). EAWAG, Dubendorf, Switzerland.]

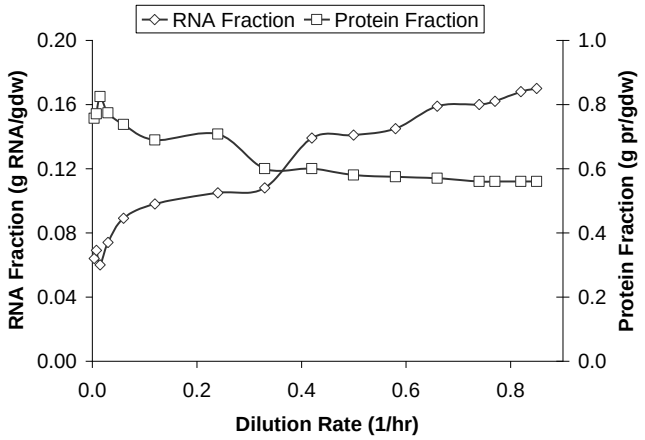

Figure 1-5. Examples of dilution rate dependence of the cellular RNA and protein content of microorganisms. Both sets of data were from *A. aerogenes* grown on minimal media. [Reprinted without permission. **Phipps, D. W. T. a. P. J.** 1967. Studies on the growth of Aerobacter aerogenes at low dilution rates in a chemostat. Microbial Physiology and Continuous Culture. Her Majesty's Stationary Office**:**240-253. (Pages 361, Figure 3).]

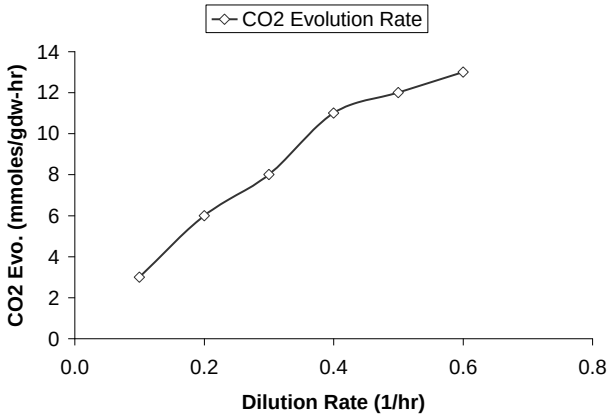

Figure 1-6. Example of dilution rate dependence of the carbon dioxide evolution rate of microorganisms. The carbon dioxide evolution rate data was from *E. coli* K-12 grown on minimal media. [Reprinted without permission. **Han, K., H. C. Lim, and J. Hong.** 1992. Acetic-Acid Formation in Escherichia-Coli Fermentation. Biotechnology and Bioengineering **39:**663-671. (Page 666, Figure 2).]

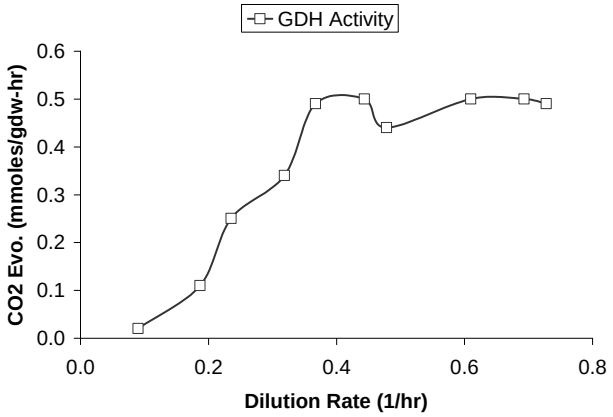

Figure 1-7. Example of dilution rate dependence of the glutamate dehydrogenase activity of microorganisms. The glutamate dehydrogenase activity was from *E. coli* W grown on minimal media. [Reprinted without permission. **Senior, P. J.** 1975. Regulation of nitrogen metabolism in Escherichia coli and Klebsiella aerogenes: studies with the continuous-culture technique. J Bacteriol **123:**407-18. (Page 413, Figure 5).]

1.5 Cellular Content and Excreted Metabolites

RNA and protein are the major cellular constituents comprising 80-85% of the dry weight of the cell. As the dilution rate increases, the RNA concentration increases at the expense of the protein concentration. Carbohydrate concentration varies markedly with the identity of the microbial species and the carbon source. For a given microbial species and carbon source, the carbohydrate content is almost independent of the dilution rate (29). Excreted metabolite concentrations also vary significantly depending on identify of the microbial species and the carbon source. Glycerol limited cultures of K. aerogenes show no measurable excretion of acetate at all dilution rates between 0.004 and 0.85 hr^{-1} (33). In contrast glucose and pyruvate limited cultures of *E. coli* show a high degree of excretion at high dilution rates (11, 16, 17).

1.6 Transients Controlled by the Transport Enzymes

The role of transport enzymes in chemostat dynamics is seen by switching the growth limiting substrate identity in the reactor feed. In this experiment a chemostat is allowed to reach

a steady state at some dilution rate and substrate feed concentration. After steady state is reached the growth limiting substrate is abruptly switched. If the transport enzymes for the new substrate are synthesized inducibly, their levels will be small when the switch occurs. Located in Figure 1-8 is an example of a transport enzyme controlled transient taken from the literature.

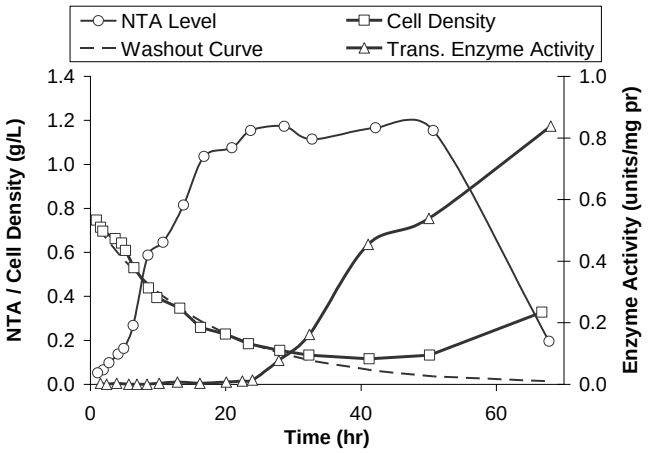

Figure 1-8. The results of glucose to nitrilotriacetate substrate switch experiment performed on a continuous culture of *Chelatobacter heintzii* grown on minimal media. [Reprinted without permission. **Bally, M., and T. Egli.** 1996. Dynamics of Substrate Consumption and Enzyme Synthesis in Chelatobacter heintzii during Growth in Carbon-Limited Continuous Culture with Different Mixtures of Glucose and Nitrilotriacetate. Appl Environ Microbiol **62:**133-140. (Page 135, Figure 2).] A theoretical washout curve was added to illustrate the predicted cell density change assuming no cell growth.

When the carbon source is switched from glucose to nitrilotriacetate (NTA) there is little to no growth for nearly twenty hours as shown by the cell density matching the theoretical washout curve during this time. The cells simply cannot take up the NTA present in the environment as shown by the lack of NTA transport enzyme activity seen during the first twenty hours. This initial lack of transport enzyme causes the substrate NTA to accumulate in the reactor until the transport enzyme reaches a level that can support growth. The transport enzyme for NTA is produced at extremely low rates under glucose limited conditions hence the low rate of transport

enzyme activity seen at the start of the experiment. The transport enzyme level is nearly zero for twenty hours and reaches fifty percent of its final value in the following twenty hours.

The rapid buildup of transport enzyme after forty hours suggests the synthesis of the enzyme is autocatalytic. Evidence from molecular biology shows that enzyme induction is not only autocatalytic, but also cooperative, since inhibition of the repressor requires that two inducer molecules to bind to it in the case of the lac operon repressor (46). Switching the growth limiting substrate from NTA to glucose produces a different transient behavior. Rapid consumption of glucose begins immediately after the switch occurs because glucose transport enzymes are constitutively produced keeping these transport enzymes at high levels even in the absence of glucose. Still little to no growth was seen for the first two to three hours of the switch from NTA to glucose (2). An appropriate question might be what is preventing the specific growth rate from adjusting instantaneously as the cell is taking up substrate yet not growing?

Similar results were found when continuous cultures of *E. coli* (43) and *K. aerogenes* (36) were subjected to a substrate switch from glucose to xylose. For many hours there was a dramatic increase in the level of xylose and a pronounced decline in the cell density. These experiments imply that when the initial level of the inducible transport enzyme is low, the transient behavior is controlled by the transport enzyme synthesis rate. There is little substrate uptake, hence little growth, until the enzyme level reaches a sufficiently high level.

1.7 Transient Dynamics Controlled by a Biosynthetic Limitation

Continuous to batch shifts of glucose limited cells reveal the role of biosynthesis in limiting microbial growth. In the experiments shown in Figure 1-9 and Figure 1-10, a sample of glucose limited cells precultured in a chemostat are immediately exposed to supersaturating concentrations of glucose in a batch reactor and the initial rates of various processes were measured. As seen in Figure 1-9 and 1-10, the growth rate and substrate uptake rate both increase

upon exposure to excess glucose regardless of the preculture dilution rate at which the cells had been growing (22). A similar response has been seen in other studies as well (28, 32). This rapid increase occurs because the transport enzymes for glucose are constitutive so they are always present at high levels. The data from the figures shows the substrate uptake rate increases to a maximal level regardless of preculture dilution rate whereas the growth rate increase is highly dependant on the preculture dilution rate. Appropriate questions here would be what is limiting the growth rate as the cell has excess substrate available and how is the cell utilizing excess substrate if it is not being channeled in to growth?

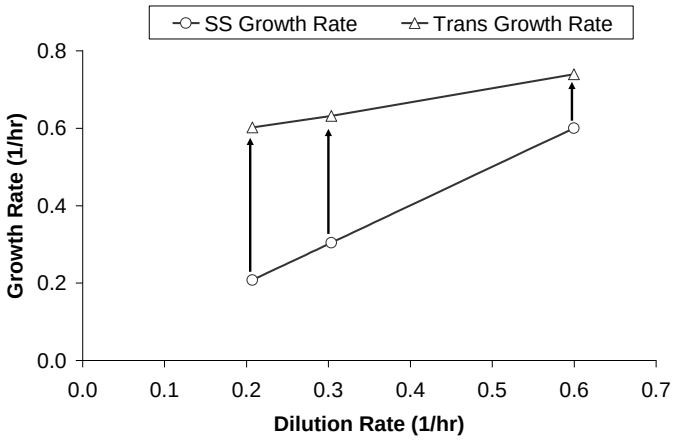

Figure 1-9. Results of a continuous to batch shift where cells of *E. coli* ML308 grown in a glucose limited chemostat on minimal media were exposed to excess glucose. The transient growth rates were measured after thirty minutes of growth. [Reprinted without permission. Lendenmann Phd dissertation (Page 72, Figure 8.1), EAWAG, Dubendorf, Switzerland.]

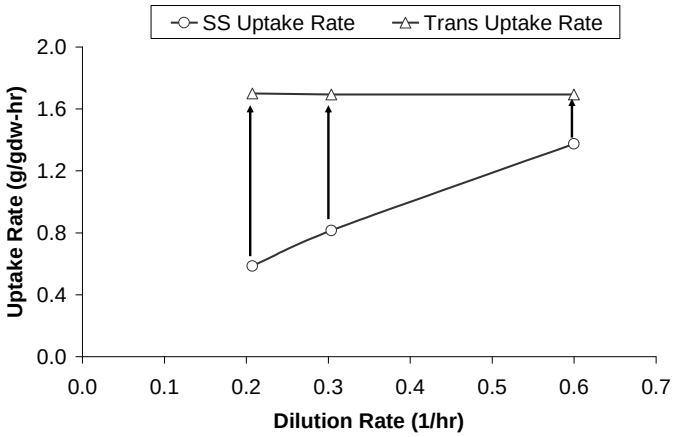

Figure 1-10. Results of a continuous to batch shift where cells of *E. coli* ML308 grown in a glucose limited chemostat on minimal media were exposed to excess glucose. The transient substrate uptake rates were measured during the first 5-7 minutes after the glucose pulse was administered. [Reprinted without permission. Lendenmann Phd dissertation (Page 72, Figure 8.1), EAWAG, Dubendorf, Switzerland.]

The specific biosynthesis rate (of RNA and protein) depends on the dilution rate at which the cells are growing before their withdrawal from the chemostat (18). This was shown in experiments where glycogenless mutants of *E. coli* B were exposed to saturating concentrations of glucose and the initial specific growth rate were measured. Since these mutants were unable to synthesize their major storage carbohydrate glycogen, the observed specific growth rate was roughly equal to the specific biosynthesis rate of only RNA and protein. Based on the measurements of the initial growth rates in these mutants it was concluded that at low dilution rates ($D<0.3\ hr^{-1}$) the specific biosynthesis rate of microbes increases rapidly but does not reach the maximum value for the strain and for high dilution rates the specific biosynthesis rate does not improve at all immediately.

It stands to reason that in wild type cells there is an absence of rapid improvement in RNA and protein synthesis at the higher dilution rates. When wild type cells of *E. coli* drawn from a chemostat are exposed to saturating concentrations of glucose the specific growth rate,

increases rapidly regardless of the dilution rate at which the cells have been growing implying that the increase is solely due to glycogen synthesis.

The synthesis of glycogen in wild type cells is not surprising. The above experiments imply that when cells growing at large dilution rates are exposed to saturating concentrations of glucose, the substrate instantly enters the cells, but cellular metabolites derived from it cannot be completely channeled in to biosynthesis of RNA and protein. A large portion must therefore be respired, excreted, or stored. The specific carbon dioxide evolution rate rapidly increases to maximal levels (levels seen at near washout dilution rates) (18, 30). The specific excretion rate (10, 12) and, if applicable, the specific glycogen synthesis rate (10, 19) increase to high levels when exposed to saturating glucose conditions. These experiments imply that if the initial level of transport enzyme is high, the transients are controlled by biosynthesis rather then by a transport limitation. There is a pronounced substrate uptake, respiration, storage, and excretion but limited or no biosynthesis until more biosynthetic capacity has been synthesized.

So what prevents the biosynthesis rate from instantly increasing to maximal levels upon exposure to excess substrate? There are two possibilities: either one or more of the biosynthetic enzymes is saturated with their substrate(s) or the ribosomes are saturated with amino acids. Substrate saturation of a biosynthetic enzyme whose product(s) are required for growth would represent a rate limiting step. Biochemical pathways necessary for growth that require the products of the saturated biosynthetic enzyme will be forced to adjust their rate of reaction based on the rate of supply of products from the saturated biosynthetic enzyme. Similarly ribosomes saturated with their amino acid substrates would also limit growth as ribosomes generate the proteins that comprise the majority of cell mass. It is generally believed that the ribosome concentration is what limits biosynthesis (5, 31); however, there is evidence to suggest that

saturation of biosynthetic enzymes, rather than ribosome concentration, prevents the biosynthesis rate from instantly increasing to the maximum level. It has been seen that the addition of amino acids to a culture results in the rapid acceleration of protein synthesis (6, 20, 24) which implies that the ribosomes are in fact not saturated with amino acids. This would suggest the limitation lies with the supply of amino acids to the ribosomes and not the ribosomes themselves.

A possible explanation for this response to increased protein synthesis upon exposure to excess amino acids could be the substrate saturation of the biosynthetic enzyme glutamate dehydrogenase (GDH). Under carbon limited conditions this enzyme is the major pathway for incorporation of inorganic nitrogen in to the cell (26, 40) and could be a limiting step in the rate of amino acid synthesis explaining why the ribosomes are not saturated. Figure 1-11 and Figure 1-12 show the transient response of RNA level and GDH activity, respectively in continuously grown microbial cells exposed to excess substrate.

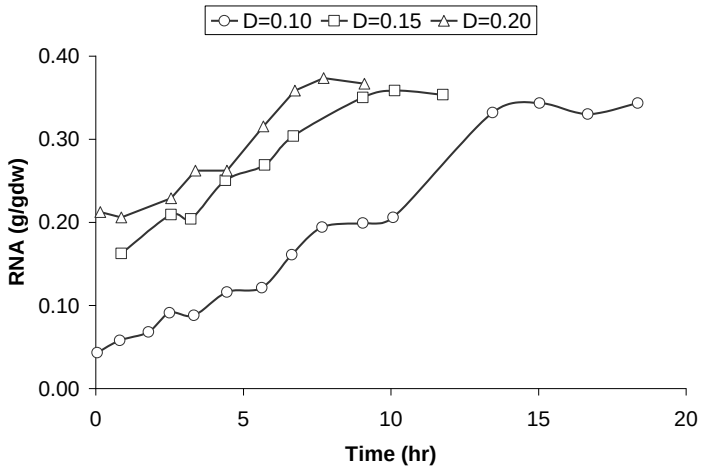

Figure 1-11. The RNA content response of continuously grown *Azobacter vinelandii* to substrate excess conditions. The bacteria were precultured on minimal media at three different dilution rates: 0.10, 0.15, and 0.20 hr^{-1}. [Reprinted without permission. **Nagai, S., Y., Nishizawa, I. Endo, and S. Aiba.** 1968. Response of a chemostatic culture of Azobacter vinelandii to a delta type pulse of glucose. J. Gen. Appl. Microbiol. **14:**121-134. (Page 125, Figure 2).]

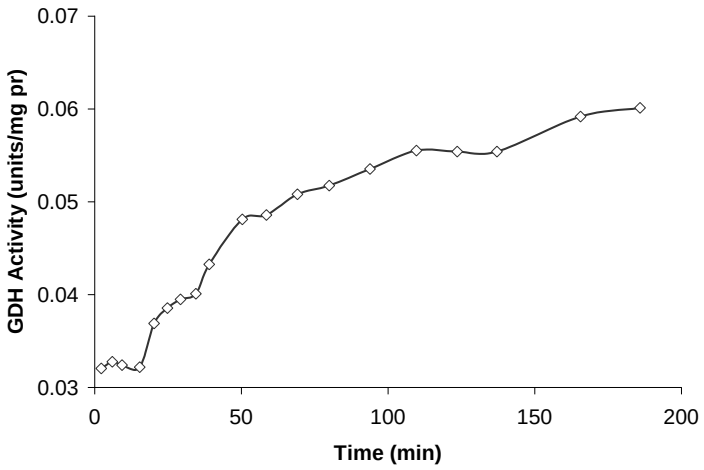

Figure 1-12. The GDH activity response of continuously grown *E. coli* W to substrate excess conditions. The bacteria were precultured on minimal media. [Reprinted without permission. **Harvey, R. J.** 1970. Metabolic regulation in glucose-limited chemostat cultures of Escherichia coli. J Bacteriol **104:**698-706. (Page 704, Figure 10).]

The slow accumulation of RNA (18, 27, 48) and GDH (18) after a continuous to batch shift follows sigmoidal kinetics. This suggests that the synthesis of GDH and RNA is autocatalytic. Such kinetics probably occur because an increase in the activity of GDH increases the level of amino acid monomers. This stimulates the production of RNA and ribosomes resulting in the synthesis of even more GDH and RNA.

1.8 Transient Response to Dilution Rate Shift Ups

In practice, chemostats regularly experience dilution rate and feed concentration shift ups. Laboratory studies have mostly been concerned almost exclusively with dilution rate shift ups. In these experiments the chemostat is allowed to reach steady state at some dilution rate and then is abruptly increased. There is substantial literature on this topic (1, 4, 9, 13, 33, 42, 43, 48), but the cellular variables were measured in relatively few studies (4, 33, 48). The cellular studies suggest that when dilution rate shift ups are small, the transients are limited by the biosynthetic machinery, and when the shift ups are large the transients are limited by transport enzymes.

Located in Figure 1-13 is the response of a glucose limited culture growing inside a chemostat to a large dilution rate shift up.

Herbert exposed a glycerol-limited culture of *K. aerogenes* to a dilution rate shift up from D=0.004 to D=0.24 hr^{-1}, which corresponds to a sixty fold increase in the substrate input rate. The transient response suggests that in the first few hours, there was a significant increase in the transport enzyme level. The initial rapid jump in the substrate uptake rate is due to saturation of the substrate uptake enzymes and the relatively slow increase after the initial jump is due to the gradual buildup of transport enzyme level because the specific substrate uptake rate is proportional to the transport enzyme level whenever the substrate concentration is saturating. The data suggests that the transport enzyme levels reach a maximum five hours after the shift up. During this time the RNA level is nearly constant. It increases significantly after the transport enzymes have peaked, and reaches the maximum more then ten hours after buildup (19).

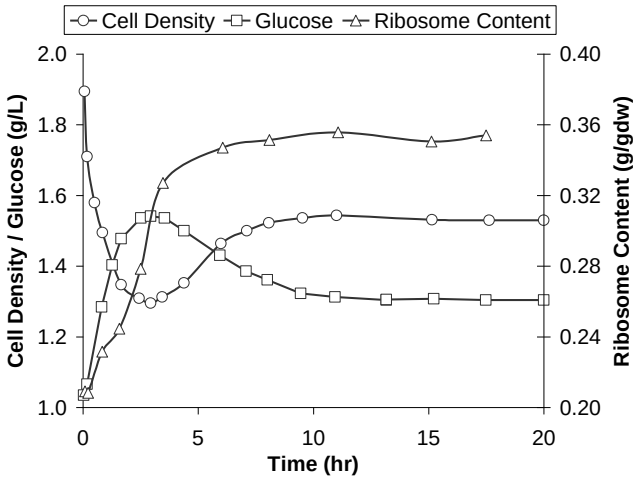

Figure 1-13. Response of a chemostat growing *E. coli* K-12 to a dilution rate shift up from D=0.2 to 0.6 hr^{-1}. Minimal media was used during the experiment. [Reprinted without permission. **Yun, H. S., J. Hong, and H. C. Lim.** 1996. Regulation of ribosome synthesis in Escherichia coli: Effects of temperature and dilution rate changes. Biotechnology and Bioengineering **52:**615-624. (Page 619, Figures 4 and 5).]

CHAPTER 2
MATERIALS AND METHODS

2.1 Growth Medium

The growth medium was prepared with deionized water in 20 L polypropylene bottles. The medium used for these experiments was a modification of a recipe used by Lendenmann et al (22). The recipe is shown in Table 2-1. Before sterilizing the medium, it was supplemented with glucose, and the pH was adjusted to 3 with concentrated H_2SO_4. The low pH prevents caramelization of the glucose during sterilization and back-contamination of the feed line during operation of the chemostat.

Table 2-1. Minimal medium recipe used for all experimentation.

Component	Conc. (M)	1L (g)
Potassium Phosphate (mono)	2.00E-02	2.7218
Ammonium Chloride	1.40E-02	0.7489
EDTA	2.20E-04	0.0819
Magnesium Sulfate Heptahydrate	2.30E-04	0.0567
Sodium Molybdate Dihydrate	1.00E-05	0.0024
Calcium Chloride Dihydrate **	1.00E-04	0.0147
Manganese Chloride Tetrahydrate	2.50E-05	0.0049
Zinc Chloride	1.25E-05	0.0017
Cupric Chloride Dihydrate	5.00E-06	0.0009
Cobalt Chloride Hexahydrate	5.00E-06	0.0012
Ferric Chloride Hexahydrate	7.50E-06	0.0020

Note: Original source was Lendenmann 1995. PhD dissertation (Page 35, Table 4.1)
Note: Adjusted reactor (not shake flask) media to pH 3 with reagent grade sulfuric acid
Note: Replaced calcium carbonate with calcium chloride due to carbonate / acid reaction
Note: Removed boric acid from media because borate adheres to the HPLC column

2.2 Bacterial Strain

The microorganism used in this study was *Escherichia coli* ML308 (ATCC 15224) obtained from the American Type Culture collection. Stock cultures were prepared by freezing cells grown on complex media that had just entered stationary phase growth. The strain was preserved at -20C in 30 ml vials containing 50% of the culture, 50% glycerol cryoprotectant, and

glass beads. The culture was resuscitated for experimental work by sterilely removing a glass bead from the stock culture and adding it to a shake flask containing the growth medium described below supplemented with 1 g/L glucose (35).

2.3 The Chemostat Setup

The chemostat cultures were grown in a 1.5 L Bioflow III fermenter (New Brunswick Scientific Co.) with a working volume of 1.2 L. The agitation speed was 1000 rpm and the aeration rate was 1.2 L/min. The bioreactor was equipped with automatic pH and temperature control. The pH was maintained at 7.0 $^{+}$/- 0.1 by addition of 1M KOH / 1M NaOH solution and 10% H_3PO_4 solutions. The temperature was maintained at 37^{o}C. The feed was pumped in by a Masterflex L/S peristaltic pump (7523-70) equipped with a Masterflex EZ Load pump head (7534-04).

2.3.1 Wall Growth Limitation

The glucose concentration in the reactor feed was kept at 200 mg/L or below. Higher feed concentrations resulted in significant wall growth within a week of inoculating the reactor. Under higher feed conditions, the initial specific growth rates after continuous mode to batch mode shifts were observed to be significantly lower than the dilution rate at which the cells had been growing in the chemostat. This probably reflects the fact that in the presence of wall growth, the steady state specific growth rate is lower than the dilution rate, since cells shearing off the wall become an additional source of cells inside the bioreactor (21). The reason for this lowering of the growth rate due to wall growth can easily be seen in the steady state cell mass balance, seen in Equation 2-1, with an extra cell source term α representing the shearing off of wall biofilm cells.

$$D \bullet C = rg \bullet C + \alpha \qquad (2\text{-}1)$$

The variables D, C, rg, and α are the reactor dilution rate, the cell density of the reactor volume, the growth rate of the cells in the bulk, and the rate of cell input in to the bulk from wall growth, respectively. If the value of α is non-zero then rg must be depressed to keep the chemostat operating at steady state. At feed concentrations of 100 mg/L of glucose, the reactor could be operated for up to month without significant wall growth.

2.3.2 Glucose Adaptation Limitation

The glucose concentration is one of the last variables to achieve a steady value inside of a glucose limited chemostat. The time scale of this transient is on the order of days suggesting a genetic adaptation to low glucose levels. This makes sense from a natural selection point of view as those cells which possess a higher capacity for uptake for the growth limiting nutrient would grow faster then cells with a lower capacity for uptake in the chemostat environment. Eventually the better adapted mutant cells would out compete and take over the reactor bulk given enough time. One such study found in the literature supported this idea (45). A deregulation mutation was found inside glucose limited *E. coli* cells grown in a chemostat that affected the transcription of a cell membrane glucose porin. Given enough time and selective pressure the cells would start producing additional glucose porin proteins that are normally not expressed under glucose limited conditions (45). These additional porins would facilitate glucose transport in to the cell and could confer a selective advantage over non-adapted cells.

A glucose adaptation experiment was conducted using the laboratory chemostat to characterize this transient in the laboratory's chemostat. Daily samples were taken from a glucose limited chemostat post a shift to D=0.6 hr^{-1}. The glucose concentration was measured and compared with a similar study found in the literature using the same strain of bacteria and a similar media composition (22). The results of this comparison are shown in Figure 2-1.

Both glucose evoluion trend lines look extremely similar with a monotonic decrease in the concentration of glucose down to the same steady value. The time it took the lab system to achieve a steady glucose concentration was four days at D=0.6 hr^{-1} or 85 cell doublings. The experiments conducted in this research were sensitive to the glucose uptake capacity thus this transient behavior introduced variation into collected data. This reproducibility problem was corrected by giving newly inoculated reactors four days time at D=0.6 hr^{-1} before any experiments were attempted to allow for microbial adaptation to low glucose levels. This operational change increased the quality of the experimental data gathered immensely.

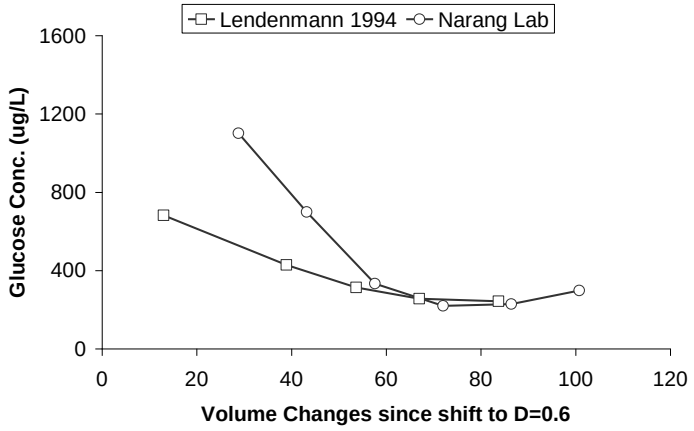

Figure 2-1 Adaptation of *E. coli* ML308 to the glucose limited chemostat environment. The cultivation used minimal media and a glucose concentration of 100 mg/L. Substrate measurements were made daily post shifting the chemostat to D=0.6 hr^{-1}. The comparison data was measured using *E. coli* ML308 grown on glucose minimal media. [Comparison data reprinted without permission. Lendenmann Phd dissertation. (Page 44, Figure 5.1). EAWAG, Dubendorf, Switzerland.]

2.4 Cell Density Measurement and Growth Rate

The concentration of cells inside the reactor at any time was determined by an absorbance measurement at 546 nm using a Spectronic Genesys 10UV spectrophotometer. In order to ensure an accurate reading the 1 ml cuvette was given approximately 45 seconds to equilibrate before the value was recorded (15). Specific growth rates of cells growing exponentially were

determined by fitting exponential curves over the time frame of interest. The fitted equation takes the form seen in Equation 2-2.

$$C = Co \bullet \exp[\mu \bullet t] \tag{2-2}$$

The variables Co, C, μ, and t are the initial cell density, final cell density, the growth rate, and time, respectively.

2.5 Sugar Measurement, Yield Determination, and Uptake Rate

Sugar concentrations were measured with a Dionex-500 HPLC equipped with an anion exchange column (CarboPac PA10) and a pulsed electrochemical detector. In this method, the sugars are ionized by using a strong base as eluent (10 mM NaOH), separated based on their differential affinity for the anion exchange column, and detected by the pulsed amperometric detector. The manufacturer's protocol resulted in a rapid increase of retention times, presumably due to adsorption of bicarbonate on the column. The addition of 1 mM $Ba(OAc)_2$ to the eluent, as recommended by (7, 8), precipitated the bicarbonate as $Ba(CO_3)_2$. The modified eluent dramatically improved the reproducibility and precision of the laboratory's sugar measurements.

The sugar biomass yield of a culture is simply the amount of cells produced per amount of sugar consumed. The biomass yield was determined for a time interval during exponential growth by plotting the cell density versus sugar concentration and using the slope of the linear fit. The final equation for yield determination during a given time interval presented as Equation 2-3.

$$Y = -(dC / dS) \tag{2-3}$$

The variables Y and (dC/dS) correspond to the biomass yield and the slope of the cell density versus sugar concentration plot. This method assumes that the biomass yield is constant over the time interval of interest. The slope of the linear fit trend line corresponds to the biomass yield

during that time interval. The specific uptake rate of sugar during the time interval was determined by dividing the specific growth by the biomass yield. The final equation for the substrate uptake rate is presented as Equation 2-4. This equation assumes that the death or decay rate of cells is negligible for the purposes of calculating the specific substrate uptake rate.

$$rs = rg / Y \tag{2-4}$$

The variables rs, rg, and Y are the specific uptake rate of sugar, the specific growth rate, and the biomass yield, respectively.

2.6 Total Cell Protein Extraction and Measurement

2.6.1 Extraction

Total cell protein was extracted using a high temperature / low pH extraction method (15). These conditions denature cellular protein and therefore the protein product could not be used for enzymatic assays. Cells were harvested via low temperature centrifugation, washed with 0.15M sodium chloride sodium citrate solution (SSC), and digested with 0.5M sodium hydroxide (NaOH) at 100^{o}C. The harsh conditions of the digestion step solubilize the cellular protein. After centrifugation, the supernatant was retained and an equivalent volume and molar strength of trichloroacetic acid (TCA) was added to adjust the pH to a neutral value.

2.6.2 Measurement

Protein detection and quantification was preformed with colorimetric detection using a bicinchchoninic acid (BCA) kit available from Pierce Biotech (34). The color change reaction occurs from amino acid (cysteine, cystine, tryptophan, and tyrosine) catalyzed reduction of Cu^{2+} to Cu^{1+}. The resulting BCA-Cu complex exhibits a strong absorbance at 562 nm that shows a near linear response with protein concentration over a broad range. Bovine serum albumin was used as a standard to generate a calibration curve for cell protein quantification.

2.7 Total Cell RNA Extraction and Measurement

2.7.1 Extraction

Total cell RNA was extracted using a cold / hot TCA treatment (15). Cells were harvested via low temperature centrifugation, washed with 0.15M SSC, and digested with 0.25 TCA at 0^{o}C. These digestion conditions lyse the cell and cause cellular RNA to precipitate as a solid. The insoluble fraction of the lysate was retained and resuspended in 0.5M TCA and placed in a 70^{o}C water bath. The treatment solubilizes RNA but leaves other macromolecules such as proteins and lipids in a solid form.

2.7.2 Measurement

RNA detection and quantification was performed with colorimetric detection using a slightly modified acidified orcinol method (23). Solutions of ferric chloride dissolved in HCl and orcinol dissolved in ethanol are combined in a 50/50 ratio and added to the extracted RNA solution generated by the cold / hot TCA treatment. The RNA in the extract reacts with acidified orcinol producing a green chromogen that exhibits a strong absorbance at 665 nm that shows a near linear response with RNA concentration. Yeast RNA was used as a standard to generate a calibration curve for cell RNA quantification.

2.8 Carbon Dioxide Evolution Measurement

The carbon dioxide evolution of the chemostat contents was measured with a Vaisala GMT222 Infrared CO_2 analyzer. The device was connected to a computer for continuous data acquisition. This was especially useful for detecting any steady state perturbations to ensure the initial conditions of the chemostat and bacteria growing within were acceptable before experiments were attempted. Special software for the CO_2 analyzer was written to allow for this continuous acquisition and recording. The code for this software appears in Appendix A.

To ensure a rapid analyzer response time to the state of the chemostat all effluent air from the reactor system was passed through the CO_2 analyzer to ensure a rapid analyzer response time to changes in the chemostat condition. The air and liquid overflow outlets were the same overflow line in the chemostat setup so an air/liquid separator was created to isolate the two phases. The overflow line was connected to a 50 mL Erlenmeyer flask with two outlets. The air phase was forced up through an exit line at the top of the flask to the analyzer while the liquid phase fell to the bottom of the flask. The liquid phase was actively pumped out to a waste tank to prevent the flask from overflowing. The setup allowed for detector response times on the order of seconds rather then minutes to changes in the chemostat carbon dioxide level. The detector output was recorded as a concentration of carbon dioxide in parts per million. The device came from the manufacturer precalibrated but was checked periodically with specially made calibration gas.

2.9 Total Organic Carbon Measurement

Total organic carbon measurements (TOC) were made with a Phoenix 8000 TOC Analyzer to quantify the amount of carbon excreted by cells in the form of organic acids or alcohols. Samples taken from the chemostat during an experiment contained excreted organic carbon as well as organic carbon from residual sugars and from the chelating agent EDTA present in the original media. The carbon contribution of the residual sugars was accounted for by first measuring the sugar concentration in the extracted sample via HPLC measurement and then subtracting the equivalent sugar carbon from a sample's TOC measurement. The carbon contribution from EDTA was accounted for by measuring the TOC of the original media (before sugar was added) and then subtracting the measured carbon from a sample's TOC. The remaining TOC of a sample was modified forms of organic carbon because there were no other known sources of organic carbon input in to the chemostat bulk.

The Phoenix 8000 TOC Analyzer used UV initiated peroxydisulfate free radical chemistry to fully oxidize organic carbon to carbon dioxide (47). A nitrogen carrier gas transports the evolved carbon dioxide to an infrared probe for detection. TOC calibration curves were generated using a glucose standard.

2.10 Elemental Content Measurement

Elemental analysis of dry cell mass was performed on a Carlo Erba-1106 Elemental Analyzer to determine the carbon content of cells for the purpose of conducting carbon balances around the laboratory chemostat. Cell mass was collected and concentrated with low temperature ($4^{o}C$) centrifugation. The resulting cell pellet was washed with cold deionized water to remove excess salts from the cell mass that could skew the elemental analysis results. The washed cell pellet was incubated overnight at $80^{o}C$ to fully desiccate the cell biomass. The resulting dry mass was pulverized to a coarse powder prior to elemental analysis.

The Carlo Erba-1106 Elemental Analyzer determined the H, N, and C content of the dry cell mass by using high temperature oxidation to convert organic H, N, and C to H_2O, NO_2, and CO_2, respectively. The evolved gases were quantified and compared with the initial dry cell mass to determine the percent content of the three elements.

2.11 Cell Disruption Techniques

In order to test the enzymatic activity of intracellular proteins, cells must be disrupted in a way that does denature or inhibit the activity of cellular proteins. Two methods were used in this research to extract proteins with little deviation from the original media pH, non-denaturing temperatures, and protease inhibitors to keep enzymatic activity as close to harvest conditions as possible.

2.11.1 Chemical Disruption

The Chemical Disruption method uses a surfactant and chicken egg white lysozyme to disrupt cells without the need for excessive mechanical force (15). First extracted cells were concentrated and washed using low temperature (4^{o}C) centrifugation and 0.15M SSC. The cell pellet was resuspended in 2 mL ice cold 50 mM Tris lysing buffer (pH=7.6) containing 100 mM NaCl, and 1 mM EDTA. This buffer has an osmolarity and pH at a level similar to chemostat conditions and more importantly will keep the pH constant during the extraction of prevent denaturing of extracted proteins. The EDTA is present to scavenge any trace heavy metals that can inactivate enzymes by adhering to active or cofactor sites on the protein. The temperature of the disruption vial was kept at 0^{o}C for the duration of the disruption procedure using an ice-water bath. A small volume (20 µl) of surfactant (10% NP-40) was then added to the suspension and vortexed vigorously (30 seconds) to permeabilize the outer membrane of the bacterial cells. The cell suspension was again centrifuged (4^{o}C) and resuspended in 0.11 ml of Tris lysing buffer. A small volume (20 µl) of sucrose solution (1.6M) was added to the disruption vial. The vial was vortexed and placed in the ice-water bath for 20 minutes. After the sucrose equilibration a small volume (43 µl) of chicken egg white lysozyme suspension (10 mg/mL) was added to the disruption vial. The vial was vortexed and placed in the ice-water bath for 20 minutes. The chicken egg white lysozyme weakens bacterial cells by degrading the peptidoglycan present in their cell walls. The sucrose added to the cell suspension prior to the lysozyme treatment helps force the lysozyme into the cell membrane holes made by the initial surfactant treatment. After the lysozyme digestion, cold deionized water (0.535 mL) was added to the cell suspension and vortexed. Next more of the surfactant, 10% NP-40 (0.179 mL), was then added to the disruption vial. Upon vortexing the suspension clears and the non-soluble components of the cell are

removed with low temperature (4^{o}C) centrifugation. The supernatant was saved and contained the solubilized cell proteins in a non-denatured state (38).

2.11.1 Chemical Disruption Drawbacks

The supernatant product from this technique is extremely viscous due to nucleic acid entanglement of liberated DNA. The viscosity of the supernatant made extracting accurate volumes with a pipette extremely difficult. Literature sources recommended sheering the crude lysate by drawing it through a syringe but this proved to be a less then ideal solution (15). The enzyme DNAse was recommended as an alternate remedy for this problem but was never implemented as a solution as there was a larger problem with the chemical disruption technique.

Of the dilution rates tested, significant cell lysis only occurred for dilution rates of 0.3 hr^{-1} or greater. When the chemical lysis technique was attempted with cells growing at D=0.1 hr^{-1}, little to no cell lysis was observed. The reason for this resistance to chemical lysing was thought to be due to the starvation response of *E. coli* (25). As the dilution rate of a carbon limited chemostat decreases the carbon substrate available to growing cells at steady state decreases as seen in Figure 1-4. Depending on the degree of starvation the cell may start activating stationary phase genes to help the organism persist in the nutrient limited environment in the hope that conditions conducive to growth will occur in the future. Formation of an extensive glycocalyx capsule around the starved cell is thought to be the source of resistance to chemical disruption (25, 29). It was hypothesized that the extensive capsule created around a starved cell provides a barrier around the cell protecting the outer membrane and cell wall from surfactant and lysozyme attack effectively preventing chemical disruption. A more effective technique was found for the disruption of highly starved cells.

2.11.1 Mechanical Disruption

The Mechanical Disruption method uses sheer forces generated by vigorously vortexing cells with micron size glass beads (3, 39). The shear force generated by the rapidly moving glass beads leads to cell disruption in even the most robust of microorganisms (37). First extracted cells are concentrated and washed using low temperature (4^{o}C) centrifugation and 0.15M SSC. Cells are resuspended in 0.3 mL of ice cold 50 mM Tris disruption buffer (pH=7.6) containing 100 mM NaCl, and 1 mM EDTA. Ice cold glass beads (100-200 μm diameter) are added to the cell suspension on a w/v basis. The cell suspension was disrupted by vortexing it vigorously for six minutes at -20^{o}C. This was achieved by placing a table top vortex inside the lab freezer and modifying the device to hold disruption vials for the purpose of hands free vortexing. The subzero temperature ensured there was no increase in temperature due to mechanical energy input that might denature the cellular proteins. The cell suspension was diluted with 0.7 mL of ice cold disruption buffer after the vortexing step. The non-soluble components of the cell were removed from the disrupted cell suspension with low temperature (4^{o}C) centrifugation. The supernatant was saved and contained the solubilized cell proteins in a non-denatured state (44).

2.11.2 Mechanical Disruption Advantages

The mechanical disruption technique solved many problems associated with the chemical disruption technique. Significant cell disruption was possible at all tested dilution rates using the mechanical technique. The resulting crude lysate from the mechanical technique had a much lower viscosity then the crude lysate from the chemical technique due simply to the shearing action of the rapidly moving glass beads allowing for more accurate volume extraction. Additionally the mechanical technique required the addition of nothing other then glass beads and a protease inhibitor solution to the cells being disrupted. The addition of surfactant, lysozyme enzyme, and other reagents in the chemical disruption technique affected the results of

the protein assay and may have had an effect on cellular enzyme activity measurements. Overall the mechanical disruption technique was superior to the chemical disruption technique for the experiments being conducted in the laboratory.

2.12 Enzymatic Assay of Glutamate Dehydrogenase

The enzyme glutamate dehydrogenase (GDH) is the protein responsible for the majority of inorganic nitrogen incorporation in *E. coli* under carbon limited conditions (26). Specifically the enzyme converts the TCA cycle intermediate α-ketoglutarate to the amino acid glutamate. The exact reaction can be seen in Figure 2-2.

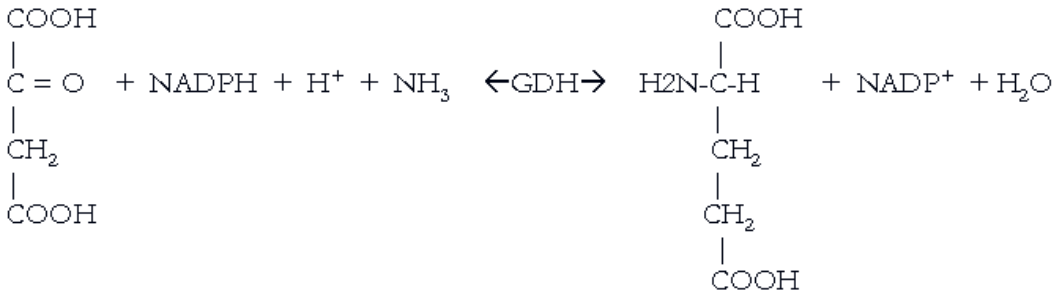

Figure 2-2 Overall reaction mechanism of the enzyme glutamate dehydrogenase. The reaction can proceed in the forward or reverse reaction depending on the concentrations of the reagents and products.

The enzymatic activity of GDH in the crude lysate extracted with the chemical and mechanical disruption methods was measured by recording the consumption of NADPH (340 nm) over 15 minutes using a Beckman DU7500 spectrometer with all reagents in excess. The enzymatic assay was performed in 1 mL cuvettes at a temperature of 25^{o}C and a pH of 7.6. The contents of the 1 mL reaction volume are shown below in Table 2-2. All reagents were made in 50 mM Tris Buffer and adjusted to pH=7.6 with 1 M HCl and 1 M NaOH.

Table 2-2. Volumes and concentrations of reagents used in the GDH assay.

Vol. (mL)	Reagent (pH=7.6)
0.6	50 mM Tris Buffer
0.1	50 mM alpha-ketoglutarate
0.1	2.5 mM NADPH
0.1	40 mM NH_4Cl
0.1	Lysate from Cell Disruption

The crude lysate showed background NADPH activity that could not be attributed to the GDH activity of the sample. Control trials, where all reagents were present except NH_4Cl, were run alongside experimental trials to account for this excess NADPH consumption activity. The net rate of NADPH consumption was used to calculate the activity of the protein samples. The activity was expressed in micromoles of NADPH consumed per minute per milligram of protein.

2.13 Deactivation and Disposal of Microorganisms

By requirement of the Environmental Health and Safety Department of the University of Florida all used media and cellular material had to be deactivated before disposal. Reactor effluent was collected in a 50 gallon waste tank and subjected to overnight chlorination before being drained in to the building water disposal system. All other cellular material was autoclaved for 15 minutes at 121^{o}C before being disposed. Any accidental spills or contamination were first deactivated with a 50% v/v ethanol/water solution before cleaning (14).

CHAPTER 3
PROTOCOL VALIDATION AND SYSTEM CHARACTERIZATION

3.1 Goals of Verification and Characterization

Before novel experiments were attempted the laboratory model system and measurements were compared with similar literature data to give credibility to the laboratory results. The steady state of a microbial chemostat provides a reproducible initial condition for the cells growing inside the reactor bulk so data collected at different reactor dilution rates was used as the basis for comparison. Collecting this steady state data also was done to characterize the initial conditions of chemostat grown cells for the purposes of future experiments. The cellular variables quantified at a range of dilution rates were the biomass yield, the protein weight percent, the RNA weight percent, the carbon dioxide evolution rate, and the initial growth and substrate uptakes rates upon exposure of the cells to excess glucose. The maximum growth rate of *E.* coli ML308 on the laboratory medium was also measured during the characterization experiments. Data from the literature that was used for comparison purposes was from systems with similar operating conditions to those of the laboratory.

3.2 Steady State Biomass Yield

The biomass yield on glucose was measured at different dilution rates and compared with data obtained using the same strain and similar media compositions (21). The two sets of data show comparable yields for matching dilution rates. The biomass yield results and comparison data appear in Figure 3-1. For the lower dilution rates (0.03-0.1 hr^{-1}) there is a sharp decrease in the yield as the dilution rate approaches zero. This trend makes sense assuming microbial cells have a minimum energy requirement for maintaining themselves. As the dilution rate decreases the energy input to the microbial cells will also decrease leaving less energy available to the cell for growth. If the energy maintenance requirement of the cell remains constant with decreasing

dilution rate then the yield must decrease as a larger percentage of consumed substrate must be used for maintenance. At the extreme case of the low washout dilution rate the cells are utilizing all consumed substrate for maintenance energy causing the yield at this point to be zero as the cells at this condition are not generating cell mass.

At intermediate dilution (0.1-0.6 hr^{-1}) rates the biomass yield keeps a relatively steady value. The maximum biomass yield occurred at a D=0.3 hr^{-1}. Beyond D=0.6 hr^{-1} the biomass yield started decreasing markedly. This trend makes sense as a chemostat will eventually washout at sufficiently high dilution rates due to the inability of cells to grow at a rate matching or exceeding the dilution rate.

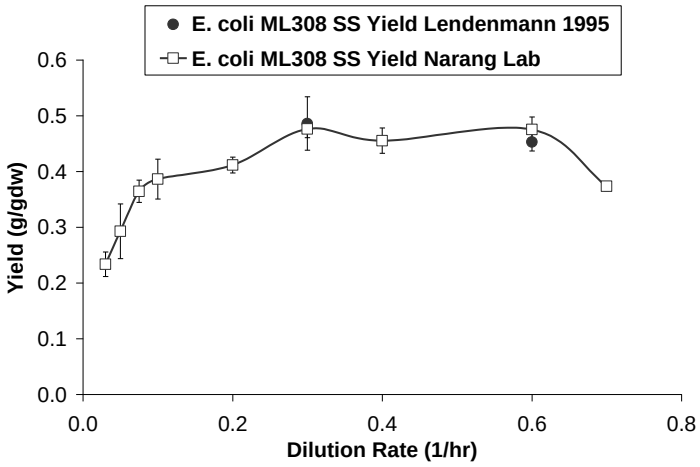

Figure 3-1. Steady state biomass yield of *E. coli* ML308 grown on 100 mg/L glucose minimal media. The biomass yield was determined by dividing the cell density by the amount of glucose utilized at different dilution rates. Specific details about cultivation and measurement appear in the Materials and Methods section. [Comparison data reprinted without permission. Lendenmann Phd dissertation (Pages 158-160, Tables B1, B2, and B3). EAWAG, Dubendorf, Switzerland.]

3.3 Carbon Dioxide Evolution Rate

The specific carbon dioxide evolution rate of *E.* coli on glucose was measured at different dilution rates and compared with similar data found for the same species grown on glucose minimal media (16). The carbon dioxide evolution rate results and comparison data used appear

in Figure 3-2. The two sets of data show similar qualitative trends. There is a linear increase in the rate of carbon dioxide evolution with respect to the dilution rate from 0.1 to 0.4 hr^{-1}. At dilution rates greater then 0.4 hr^{-1}, the carbon dioxide evolution rate slows considerably.

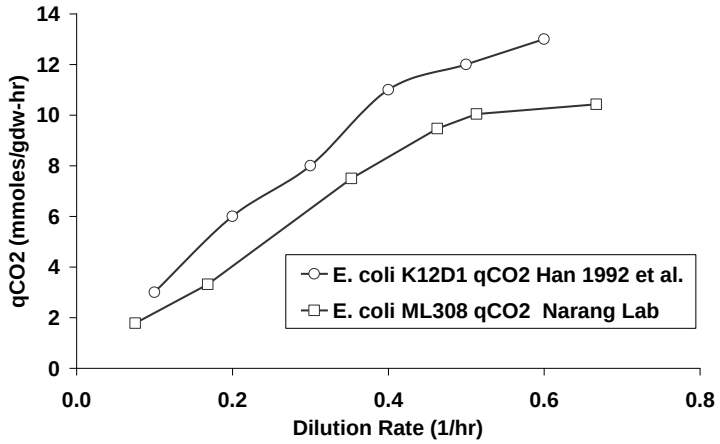

Figure 3-2. Steady state carbon dioxide evolution rate of *E. coli* ML308 grown on 100 mg/L glucose minimal media. Specific details about cultivation and measurement appear in the Materials and Methods section. The effluent air carbon dioxide concentration, the chemostat bulk cell density, and the air flow rate were used to calculate a specific evolution rate. [Comparison data reprinted without permission. **Han, K., H. C. Lim, and J. Hong.** 1992. Acetic-Acid Formation in Escherichia-Coli Fermentation. Biotechnology and Bioengineering **39:**663-671. (Page 666, Figure 2).]

3.4 Protein and RNA Dry Weight Fractions

The protein content of *E. coli* ML308 was measured at different dilution rates and compared with the results of a similar study done with a different strain of bacteria grown on glucose minimal media. Unfortunately no data was found for the dilution rate dependence of *E. coli* protein content for similar conditions. The results of the protein dry weight fraction measurements and the comparison data used appear in Figure 3-3. The protein fraction was a decreasing function of the dilution rate ranging from 76% (at D=0.1 hr^{-1}) to 61% (at D=0. 7). The data used for comparison matched the trend observed in the laboratory extremely well despite being collected using a different species of bacteria.

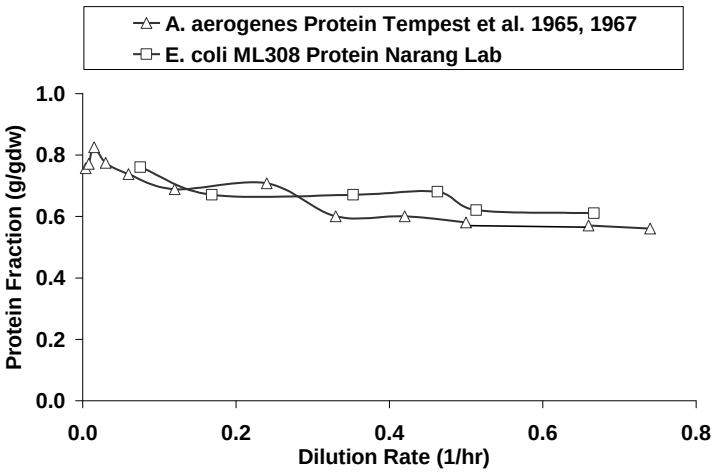

Figure 3-3. Protein dry weight fraction of *E. coli* ML308 grown on 100 mg/L glucose minimal media. Specific details about cultivation and measurement appear in the Materials and Methods section. The comparison data was measured using *A. aerogenes* grown on glucose minimal media [Comparison data reprinted without permission. **Phipps, D. W. T. a. P. J.** 1967. Studies on the growth of Aerobacter aerogenes at low dilution rates in a chemostat. Microbial Physiology and Continuous Culture. Her Majesty's Stationary Office**:**240-253. (Pages 361, Figure 3).]

The RNA content of *E. coli* ML308 was measured at different dilution rates and compared with data from the same comparison data set. The RNA fraction results appear in Figure 3-4. The RNA fraction was an increasing function of the dilution rate ranging from 12% (at D=0.1 hr^{-1}) to 16% (at D=0. 7). The data used for comparison was a monotonic increasing trend as well but had a low RNA content at lower dilution rates that increased at faster rate. At a dilution rate of 0.7 hr^{-1} the RNA level of both data sets had similar values. The difference in RNA trends could be a result of the fact the two trends collected were from different species of bacteria.

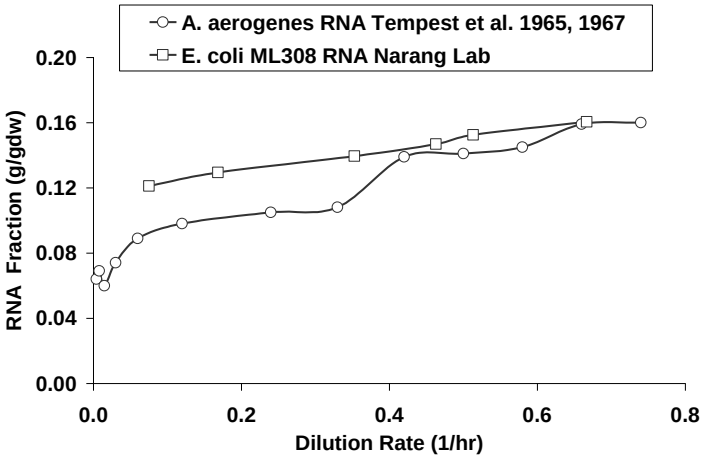

Figure 3-4. RNA dry weight fraction of *E. coli* ML308 grown on 100 mg/L glucose minimal media. Specific details about cultivation and measurement appear in the Materials and Methods section. The comparison data was measured using *A. aerogenes* grown on glucose minimal media. [Comparison data reprinted without permission. **Phipps, D. W. T. a. P. J.** 1967. Studies on the growth of Aerobacter aerogenes at low dilution rates in a chemostat. Microbial Physiology and Continuous Culture. Her Majesty's Stationary Office**:**240-253. (Pages 361, Figure 3), Microbiological Research Establishment, Porton, Salisbury, Wilks, UK.]

3.5 Maximum Specific Growth Rate on Minimal Media

The maximum specific growth rate is the highest speed of cell division a microbial species can obtain on a given media at a specific pH, temperature, etc. All nutrients in the medium are at saturating concentrations with respect to the growing cells. The maximum growth rate on a particular medium is generally unique for different microbial species. Exposure of nutrient limited cells to excess nutrients will not result in an immediate adjustment of the cell specific growth rate to the maximal value. There is an adaptation period, on the order of days, for the cells to achieve their maximum speed of cell division (21).

The maximum specific growth rate of *E. coli* ML308 was determined and compared with a value published for the same strain and similar media composition (21). A population of *E. coli* was constantly exposed to a nutrient surplus (1 g/L glucose) for five days by sterile subculturing. The cells were never allowed to enter stationary phase for the duration of the experiment. After

five days the culture was growing at a growth rate of ~0.91 hr^{-1} which compared well with the value 0.92 hr^{-1} found in the literature.

3.6 Initial Growth and Uptake Rate Response to Nutrient Excess

Chemostat grown glucose limited cells rapidly increase their growth rate and substrate uptake rate upon exposure to saturating glucose concentrations. The level of increase for the growth rates and uptake rates were dependant on the preculture dilution of the chemostat grown cells. The initial growth rate and uptake rates of *E. coli* ML308 growing at different dilution rates were determined by measuring the cell density and glucose concentration of a culture exposed to excess glucose. Reactor volume (50 mL) from a glucose limited chemostat was extracted and transferred to a pre-warmed shake flask (250 mL) and inoculated with a saturating concentration of glucose (50 mg/L). The shake flask was then placed in a tabletop shaker (2000 RPM, 37^{o}C) and the cell density and glucose level were measured every five minutes for thirty minutes. The growth and uptake rates were calculated as described in the Materials and Methods section.

The results of the initial rate experiments for three different dilution rates as well as comparison data from similar experiments taken from the literature (21) appear in Figure 3-5 and Figure 3-6. The arrows indicate the increase in growth or uptake rate upon the shift from glucose limited continuous mode growth to glucose surplus batch mode growth. At all dilution rates tested both the substrate uptake rate and growth rate increased upon exposure to excess glucose. The growth rates compare well with the results of similar experiments done with the same species. The initial growth rates of cells growing at dilution rates less then 0.1 hr^{-1} have never been explored to the best of our knowledge. The increase in the growth rate upon exposure to excess glucose dropped considerably as the dilution rate approached zero. The highly starved cells were unable to maintain the capacity for increased growth upon exposure to nutrient excess.

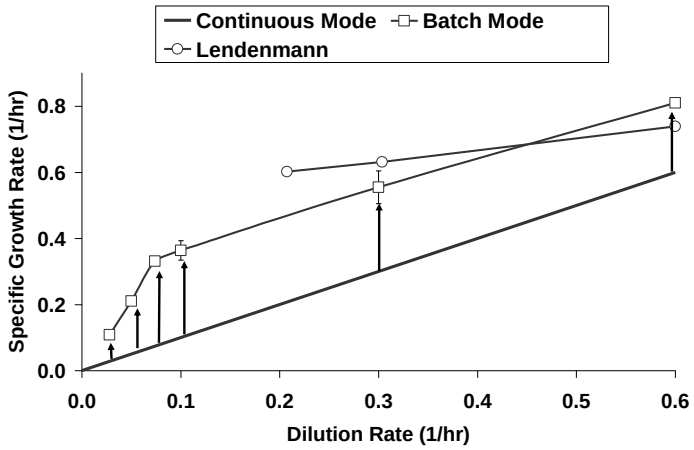

Figure 3-5. Initial growth rate increase of *E. coli* ML308 grown on 100 mg/L glucose minimal media upon exposure to excess glucose (50 mg/L). The growth rate under steady state conditions appears as the solid line. Specific details about cultivation and measurement appear in the Materials and Methods section. The comparison data was measured using *E. coli* ML308 grown on glucose minimal media. [Comparison data reprinted without permission. Lendenmann Phd dissertation (Page 72, Figure 8.1), EAWAG, Dubendorf, Switzerland.]

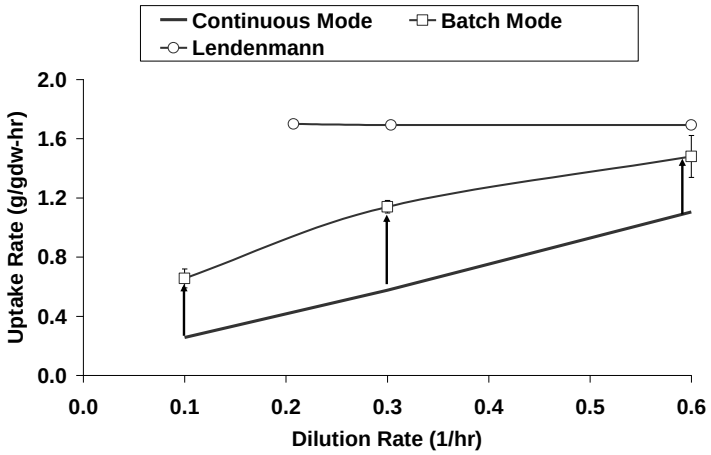

Figure 3-6. Initial uptake rate of *E. coli* ML308 grown on 100 mg/L glucose minimal media upon exposure to excess glucose (50 mg/L). The uptake rate under steady state conditions appears as the solid line. Specific details about cultivation and measurement appear in the Materials and Methods section. The comparison data was measured using *E. coli* ML308 grown on glucose minimal media. [Comparison data reprinted without permission. Lendenmann Phd dissertation (Page 72, Figure 8.1), EAWAG, Dubendorf, Switzerland.]

The substrate uptake rates of the two different data sets had noticeable differences. The collected substrate uptake rates were lower then the comparison data but it has been hypothesized that the reason for this discrepancy is the timescale on which the substrate uptake rates were measured. Lendenmann (1995) collected glucose samples over a seven minute period as opposed to over a thirty minute period. The reasoning for this discrepancy could be the specific growth rate oscillations discussed in Chapter 5 and shown in Figure 5-5. If the specific growth rate of the bacterial cells oscillates with time then the specific substrate uptake rate could be oscillating as well.

3.7 Concluding Remarks

These characterization experiments were necessary to ensure the validity of the new protocols and our model system. In all cases the results collected were comparable to those from similar experiments done by other researchers. In addition the data from these experiments provided a benchmark for the future experiments. The chemostat steady state data collected characterized the initial state of cells of *E. coli* growing at different glucose limited growth rates. These benchmarks were checked routinely before conducting experiments to ensure the state of the chemostat grown cells were correct so reproducible data would be collected.

CHAPTER 4
STEADY STATE AND TRANSIENT CARBON FLUX

4.1 Introduction

The transient response of a microbial chemostat is a challenge facing biology and engineering today. Continuously run bioreactors are inevitably disturbed with fluctuations in their feed flow rate that can lead to lengthy transients involving massive cell loss and an overshoot in the limiting substrate concentration. These long transients can lead to product deterioration in industrial bioreactors and violations at wastewater treatment facilities. Characterizing the initial carbon flux of these continuously cultivated microorganisms after one of these perturbations is the goal of this research. This knowledge could help in the development of a better model that could mitigate the effects of these reactor transients. A literature search yielded no systematic study of the transient carbon flux of continuously grown microorganisms at a range on carbon limited growth rates.

Exposure of glucose limited cells to saturating concentrations of glucose will rapidly increase their specific growth rate and specific substrate uptake rate. As seen in Figure 3-5 and Figure 3-6 the substrate uptake rate increase appears to be independent of the preculture dilution rate at $D=0.3\ hr^{-1}$ and above but the increase in growth rate appears to change linearly with dilution rate. The cells are consuming increased amounts of substrate at all dilution rates tested yet grow at different rates. An appropriate question here would be how are cells utilizing this excess substrate if it is not being channeled into production of more cells?

Microorganisms growing under aerobic conditions generally have three ways they can utilize consumed carbonaceous substrate. They can channel the carbon in to synthesis of cell biomass (biosynthesis), fully oxidize the organic carbon to carbon dioxide for energy (respiration), or partially catabolize the substrate and discharge the product in to the environment

around the cell (excretion). All three of these cellular carbon sinks for consumed carbonaceous substrate were measured during steady state growth and during transient growth immediately following removal of the substrate limitation. The measurements were conducted at D=0.1, 0.3, and 0.6 hr^{-1} to see the change in carbon flux response at a range of glucose limited preculture growth rates.

4.2 Materials and Methods

4.2.1 Organism and Cultivation Conditions

The organism used in this work was *E. coli* ML308 (ATCC 15224) obtained from the American Type Culture collection. Cells were resuscitated from a frozen stock culture overnight on glucose (1 g/L) minimal media. The minimal media used in this work was described in the Materials and Methods Chapter and the components of which appear in Table 2-1. The chemostat cultures were grown in a 1.5 L Bioflow III fermenter (New Brunswick Scientific Co.) with a working volume of 1.2 L. The agitation speed was 1000 rpm and the aeration rate was 1.2 L/min. The bioreactor was equipped with automatic pH and temperature control. The pH was maintained at 7.0 $^{+}$/- 0.1 by addition of 1M KOH / 1M NaOH solution and 10% H_3PO_4 solutions. The temperature was maintained at 37^{o}C. The feed was pumped in by a Masterflex L/S peristaltic pump (7523-70) equipped with a Masterflex EZ Load pump head (7534-04). The reactor was equipped with a Vaisala GMT222 CO_2 analyzer for continuous monitoring of the carbon dioxide output of the reactor.

Chemostat cultures were precultured on glucose (100 mg/L) for four days at D=0.6 hr^{-1} before shifting to the trial dilution rate to ensure adaptation of the *E. coli* cells to low glucose conditions for reasons described in the Materials and Methods Chapter. The chemostat was then allowed to equilibrate for ten additional residence times to ensure the cells were adjusted to the new growth conditions (21). The cellular carbon dioxide evolution rate of the reactor was

monitored during the adaptation and equilibration phases of preculturing to ensure the history and consequently the initial state of the chemostat grown cells were correct before attempting an experiment.

4.2.2 Carbon Measurement Methodology

The carbon content of cell mass inside the reactor at any time was estimated using a carbon mass fraction of cell dry weight conversion factor. The concentration of cells inside the reactor at any time was determined by an absorbance measurement at 546 nm using a Spectronic Genesys 10UV spectrophotometer. This carbon content conversion factor was found by measuring the steady state carbon mass fraction using a Carlo Erba-1106 Elemental Analyzer at six different dilution rates (0.1-0.6 hr^{-1}). Cell mass was collected, concentrated in a centrifuge (5,000 RPM, 4^{o}C), desiccated overnight in an 80^{o}C oven, and then pulverized to a fine powder prior to analysis. The carbon mass fraction of the cell dry weight was assayed three times with this method to ensure an accurate conversion factor. The steady state carbon fraction of the dry cell weight for the different steady states appears in Figure 4-1. This conversion factor was used to calculate the carbon content of cell biomass of the chemostat at any time as shown in Equation 4-1.

$$Cb = CF \bullet C \tag{4-1}$$

The variables Cb, CF, and C in Equation 4-1 correspond to the cell biomass carbon content of the chemostat (units mg C/L), the carbon weight fraction of cell mass of steady state cells at the preculture dilution rate (units g C/mg), and the cell density of the chemostat volume (units mg /L), respectively.

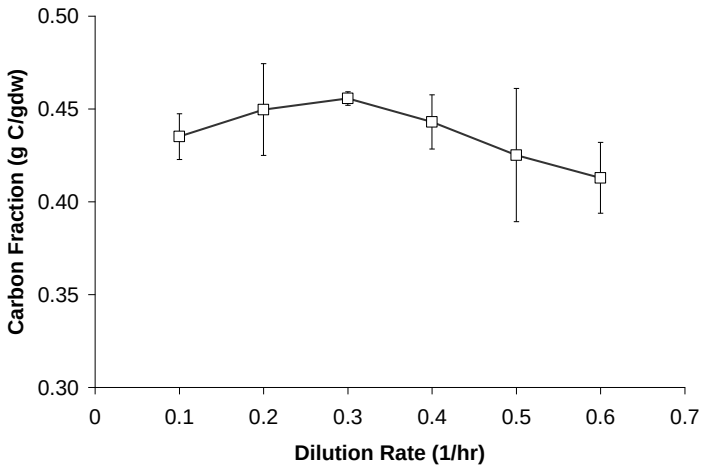

Figure 4-1. Carbon mass fraction of dry weight *E. coli* ML308 grown at different glucose limited dilution rates. The analysis was performed on a Carlo Erba-1106 Elemental Analyzer.

The carbon content of the effluent air was determined with output from the Vaisala GMT-222 CO_2 analyzer and associated software as described in the Materials and Methods Chapter. The cell specific respiration rate calculated using Equation 2-1 was a five minute average of CO_2 values centered on the time a cell density measurement was taken. The rate of evolution was converted to milligrams of carbon respired per liter of reactor volume by the conversion shown in Equation 4-2.

$$Cr = 12 \bullet qCO2 \bullet C \bullet dt \tag{4-2}$$

The variables Cr, qCO2, C, and dt in Equation 4-2 correspond to the respired carbon evolved over the dt time period (units mg C/L), the cell specific CO_2 evolution rate (units mmoles C/mg-hr), the cell density of the chemostat (units mg/L), and the time interval (unit hr), respectively.

The carbon content glucose and excreted products in the chemostat bulk were determined with a Dionex DX-500 HPLC and a Phoenix 8000 TOC Analyzer. The details of how these measurements were performed appear in the Materials and Methods Chapter. Little manipulation

was needed to convert the glucose concentration and excreted carbon concentration to the correct form (units mg C/L) necessary for analysis.

4.2.3 The Continuous to Batch Shift Experiment

The continuous to batch shift of a chemostat was achieved by simple switching off the feed pump. To simulate the environment a microbial cell experiences during a dilution rate shift up, a 50 mg/L pulse of glucose was injected in to the reactor bulk immediately following the shift from continuous to batch mode. Shifting the chemostat to a batch reactor was necessary for data collection as extraction of large sample volumes were necessary for measuring the total organic content of the reactor bulk as kinetics of batch growth are independent of the active volume of the reactor. Frequency of variable measurement, sample collection, and approximate volumes taken for measurement appear in Table 4-1.

Table 4-1. Frequency of data collection and approximate reactor volume taken for each measurement during the continuous to batch shift experiments. Sample extraction for the total organic carbon measurement only applied during batch mode growth as significant reactor volume was required. Steady state TOC samples were only taken immediately before the shift from continuous to batch mode.

Variable	Vol. (ml)	Freq. (min)
Cell Density	6	5
CO2 Conc.		1
Glucose	2	10
TOC	20	10

To observe the change in carbon utilization pattern during a pseudo dilution rate shift up, most of the steady state variables were monitored for an hour prior to the continuous mode to batch mode shift. After the 50 mg/L pulse of glucose was added to the reactor the indicated variables were monitored until exhaustion of glucose denoted by a sudden, rapid decrease in the carbon dioxide concentration and an unchanging reactor cell density.

To ensure the validity of collected data at least 90% of the added glucose carbon was accounted for in either the generated cell biomass, respired carbon dioxide, and in excreted organic carbon both during continuous mode growth and at the end of batch mode growth. Each dilution rate was tested at least twice to ensure a reproducible trend.

4.3 Results

Figure 4-2, Figure 4-3, and Figure 4-4 show example data from each of the three preculture dilution rates tested. Figure 4-5 shows a comparison in the cell density trends among the three different preculture dilution rates and Figure 4-6 shows a comparison in the specific CO_2 evolution rate trends among the three dilution preculture dilution rates. Table 4-2 shows numerical values for growth rate, substrate uptake rate, CO_2 evolution rate, and biomass yield before and during batch mode growth.

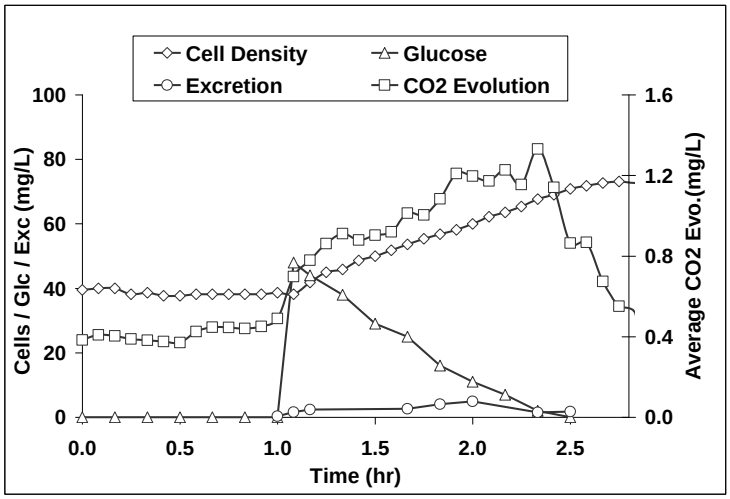

Figure 4-2. Results of a continuous to batch shift of a bioreactor growing *E. coli* ML308 continuously at D=0.1 hr^{-1} on 100 mg/L glucose minimal media. Batch mode shift and injection of ~50 mg/L glucose occurred at 1 hour.

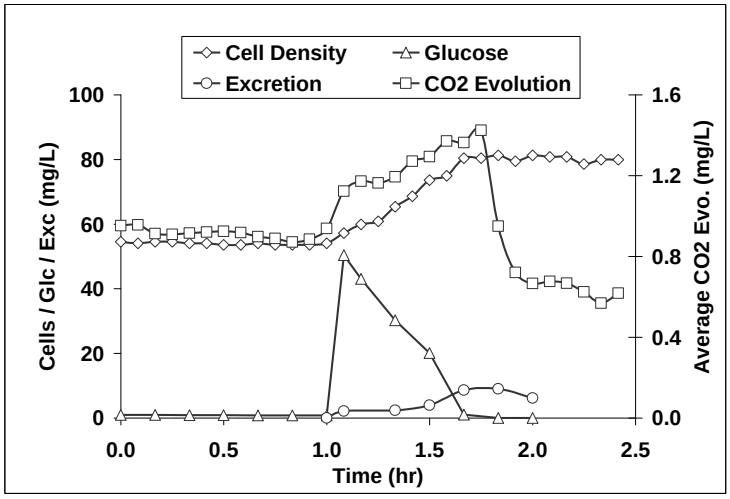

Figure 4-3. Results of a continuous to batch shift of a bioreactor growing *E. coli* ML308 continuously at D=0.3 hr^{-1} on 100 mg/L glucose minimal media. Batch mode shift and injection of ~50 mg/L glucose occurred at 1 hour.

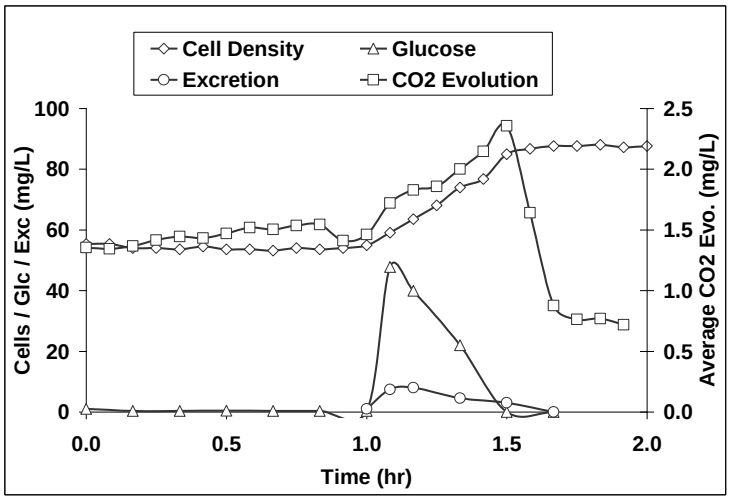

Figure 4-4. Results of a continuous to batch shift of a bioreactor growing *E. coli* ML308 continuously at D=0.6 hr^{-1} on 100 mg/L glucose minimal media. Batch mode shift and injection of ~50 mg/L glucose occurred at 1 hour.

At every dilution rate tested there was a seemingly immediate increase in substrate uptake rate and growth rate. The dilution rate D=0.6 hr^{-1} attained higher overall growth rates and carbon dioxide evolution rates as seen in Figure 4-5 and Figure 4-6. The greatest increase in growth rate,

substrate uptake rate, and carbon dioxide evolution rate were found at the dilution rate D=0.1 hr^{-1} as seen in Table 4-2.

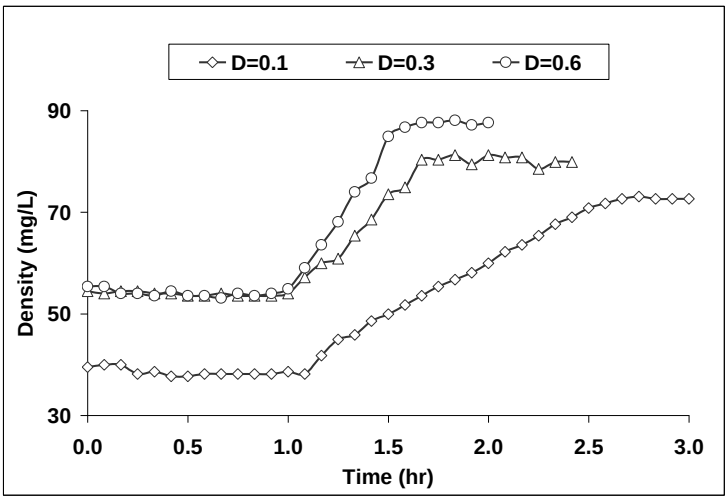

Figure 4-5. Comparison of the cell density evolution of the three preculture dilution rates before, during, and after the continuous to batch shift.

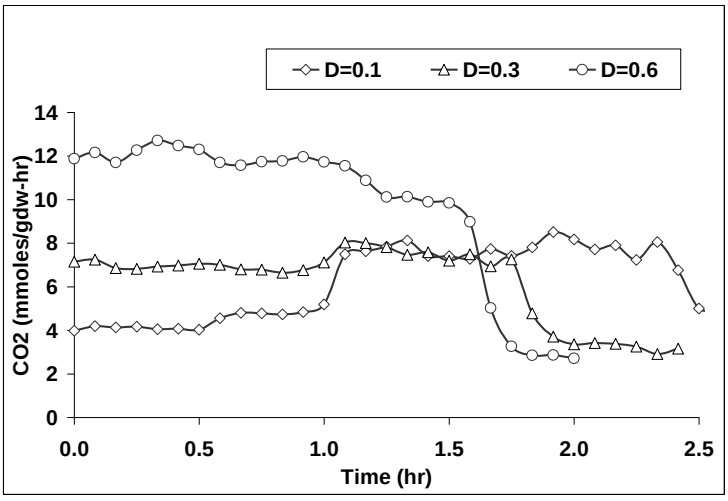

Figure 4-6. Comparison of the cell density evolution of the three preculture dilution rates before, during, and after the continuous to batch shift.

Table 4-2. Growth rate, uptake rate, carbon dioxide evolution rate, and biomass yield before and during a batch mode shift for the six different trials.

D (1/hr)	Cont. rg (1/hr)	Batch rg (1/hr)	Cont. rs (1/hr)	Batch rs (1/hr)	Cont. Y (gdw/g)	Batch Y (gdw/g)	Cont. qCO2 (mm/g-hr)	Batch qCO2 (mm/g-hr)
0.10	0.10	0.38	0.26	0.61	0.40	0.54	4.85	8.06
0.10	0.10	0.33	0.25	0.70	0.39	0.54	4.42	7.73
0.30	0.30	0.52	0.60	1.17	0.54	0.45	6.93	7.53
0.30	0.30	0.59	0.55	1.11	0.54	0.53	7.70	11.44
0.60	0.60	0.81	1.08	1.38	0.55	0.59	10.93	11.45
0.60	0.60	0.81	1.13	1.58	0.53	0.52	11.96	10.20

It is worth mentioning that at D=0.1 hr^{-1} there is an increase in yield upon exposure to excess glucose while at D=0.3 and 0.6 hr^{-1} the batch mode yield stays relatively constant. This was unexpected as other studies looking into transient yields after a dilution rate shift up show a marked drop in the yield (13). The experiments in question had transients that operated on a much longer time scale then the transients in this study and was thought to be the cause of the yield discrepancy. Simple shake flask experiments done at the three different dilution rates using 1 g/L glucose confirmed that the yield does decrease at all dilution rates on a longer time scale.

As stated earlier at least 90% of the injected glucose was accounted for in carbon balances done at steady state and upon the exhaustion of glucose during batch mode growth. Carbon utilization by cells does change under substrate excess conditions and varies with preculture dilution rate. A comparison of carbon utilization between steady state growth and transient growth appears in Figure 4-7.

During steady state growth at D=0.1 hr^{-1} about 50% of the consumed glucose went to respiration and 50% is going to biosynthesis. During excess glucose conditions most of the consumed carbon is channeled towards biosynthesis resulting in the much higher yield seen during batch growth. Little excretion is seen during steady state and transient growth at D=0.1 hr^{-1}. At D=0.3 hr^{-1} the split between biosynthesis and respiration was 64% and 39%, respectively. During substrate excess conditions the fraction of consumed carbon being used for growth stays

relatively constant while the fraction being excreted increases immensely. At D=0.6 hr^{-1} the trend is different still. This dilution rate shows the least amount of change upon exposure to excess glucose. The fraction of carbon being utilized during steady state and transient growth stays roughly the same before and after the shift at 66% being used for biosynthesis and 27% being respired to carbon dioxide. While the cells did excrete organic compounds during batch growth, they were completely consumed by the end of the transient (including some leftover excretory products from steady state growth).

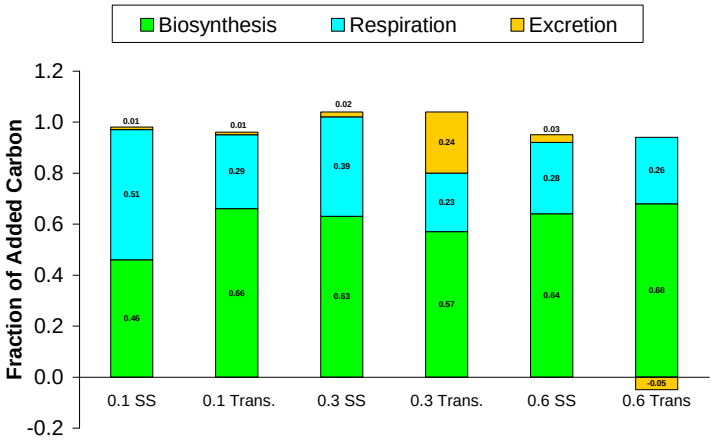

Figure 4-7. A comparison of cellular carbon utilization pattern during continuous mode growth and during batch mode growth for D=0.1, D=0.3, and D=0.6.

4.4 Discussion

The most glucose starved dilution rate, D=0.1 hr^{-1}, was extremely efficient at incorporating consumed substrate into biomass. A sizable increase in the amount of carbon going toward biosynthesis is observed upon exposure to excess glucose leading to a higher yield. Little to no excretion was seen during batch growth. For the intermediate dilution rate, D=0.3 hr^{-1}, the bacteria were less starved during the preculturing phase which proved to make them more wasteful in terms of carbon utilization. Cells growing at this dilution rate utilized the same

percentage of consumed substrate in biosynthesis during glucose limited growth and glucose excess growth. There was an increase in the carbon dioxide evolution rate, but a large percentage of the consumed substrate during transient growth was excreted back in to the medium. This suggests saturation of respiration and biosynthetic capacity forcing the cell to excrete the excess consumed substrate as partially catabolized organic molecules. The cells precultured at D=0.3 hr^{-1} did not utilize the excreted organic products before exponential growth ended. Cells growing at the highest dilution rate tested, D=0.6 hr^{-1}, were least affected by the excess glucose conditions. Carbon accounting at the end of the exponential growth phase showed the excess carbon was utilized by the cell in percentages proportional to those seen at steady state. At D=0.6 hr^{-1} there was little or no increase in the carbon dioxide evolution rate leading to the same trend seen at D=0.3 hr^{-1} where the cells tend to excrete a large fraction of the consumed substrate. The excreted organic products were completely consumed by the end of the exponential growth phase signifying that cells grown at D=0.6 hr^{-1} have a higher capacity to utilize their excretory products than the intermediate dilution rate of D=0.3 hr^{-1}. In conclusion as the preculture growth rate (and consequently degree of glucose availability) increases there tends to be less excess capacity for respiration and growth leading to more excretion of excess consumed carbon. Only at the highest dilution rate of D=0.6 hr^{-1} were the bacteria able to utilize the excreted compounds before the transient ended.

The steady state and transient yields support the idea that as preculture dilution rate increases the capacity for excess growth and respiration decreases. At D=0.1 hr^{-1} the steady state yield is significantly lower then those seen at D=0.3 hr^{-1} and D=0.6 hr^{-1}. The higher dilution rates show an equivalent and higher yield. This suggests that cells growing at D=0.1 hr^{-1} inside a chemostat have to use more of their consumed substrate for the production of energy

(respiration) than in biosynthesis unlike the higher dilution rates. This idea is also supported by the fact that little to no excretion is seen during steady state growth at D=0.1 hr^{-1} as the cell is either fully oxidizing carbon for energy or incorporating it in to cell biomass. Upon exposure of cells growing at D=0.1 hr^{-1} to excess glucose, the cells increase the fraction of consumed carbon going to biosynthesis to levels seen at D=0.3 hr^{-1} and D=0.6 hr^{-1}. This suggests that cells keep an excess capacity to grow at their desired yield under starved conditions. This trend probably does not hold at dilution rates less then D=0.1 hr^{-1}. There is a drastic decrease in the glucose excess growth rate seen at extremely low dilution rates, as seen in Figure 4-5, as more substrate is needed for energy production just to maintain the cell. The capacity for excess growth starts decreasing markedly below D=0.1 hr^{-1} as the microbial cells become increasingly starved.

In all cases the initial transient yield on the time scale measured increased or remained constant upon exposure to excess glucose. This is in contrast to what has been seen in the literature. Others have seen that exposure of substrate limited microorganisms to excess substrate leads to an overall decrease in the yield during transient growth. Shake flask experiments done with higher concentrations of inoculated glucose revealed that the yield does indeed decrease on a much longer time scale. So there appears to be an initial yield increase on a fast time scale and a decrease on a longer time scale. The cause of this yield variation with time is yet to be determined

CHAPTER 5
ATTEMPT TO IDENTIFY THE BIOSYNTHETIC LIMITATION

5.1 Introduction

The inability of microbial cells, growing under carbon limited conditions, to instantly adjust their growth rates to maximal levels has been seen in the literature and from data collected in previous experiments. Currently the concentration of ribosomes inside microbial cells is thought to be the cause of the intracellular growth limitation and is used as such for modeling purposes (5). At different preculture dilution rates the initial increase in the growth rate upon exposure to excess substrate has been found to be a linearly increasing function of the dilution rate much like the ribosome level. Since ribosomes are necessary for the production of protein; which constitutes the majority of cell biomass, one can easily draw the conclusion that ribosome levels control the growth rate during a dilution rate shift up. Experimental data collected where the growth rate and ribosome level have been monitored simultaneously certainly suggest this is the case. Figure 5-1 is a dilution rate shift up experiment conducted where the cell specific growth rate and the RNA level of the cell were recorded during transient growth.

The majority of cellular RNA (97%) is ribosomal RNA making total RNA content a good indirect measure of ribosome content (29). Clearly the cell specific growth rate and RNA level are a good qualitative match; however, there are lines of evidence to suggest that the ribosome content of a cell is not the true intracellular biosynthetic limitation.

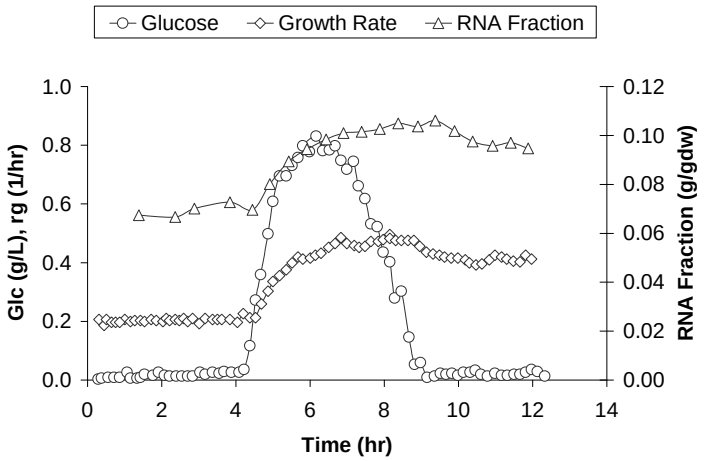

Figure 5-1. Example dilution rate shift up (0.075 to 0.409 hr^{-1}) from the literature where the growth rate and RNA level were measured versus time. The microorganism used was *Lactococcus cremoris* grown on glucose minimal media. [Reprinted without permission. **Benthin, S., and J. Villadsen.** 1991. Growth energetics of Lactococcus cermoris FD1 during energy-carbon and nitrogen limitation in steady state and transient cultures. Chem. Eng. Sc. **49:**589-609. (Page 4237, Figure 5).]

The well known fact that microbial cells grow much faster on complex media than on minimal media should already be enough evidence to show that the ribosome content of a cell cannot be the true biosynthetic growth limitation seen in carbon limited microbial cells. Analysis of data from the literature seems to suggest that the biosynthetic limitation is actually a result of a lack of amino acids. Figure 5-2 is a comparison of transient growth rates among cultures of *E. coli* grown under different preculture conditions and transient conditions. Cells extracted from a carbon limited chemostat and exposed to excess glucose and excess amino acids produced growth rates that exceeded even the maximum growth rate attainable on minimal media alone. The ribosomes of microbial cells exposed to excess glucose are most likely unsaturated with their amino acid substrates making the supply of amino acids to the ribosomes and not the ribosome level itself the cause of the biosynthetic limitation.

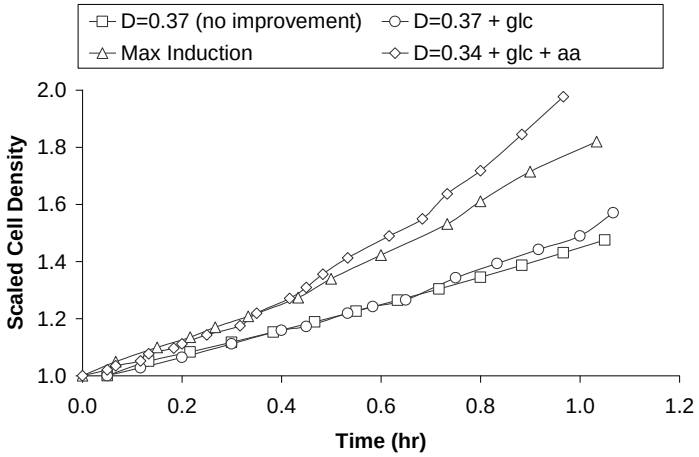

Figure 5-2. Example data from the literature showing that amino acids limit the growth of carbon limited cells exposed to excess glucose. The microorganism used was *E. coli B* precultured on glucose limited minimal media. The open box trend refers to cells growing at D=0.37 that would show no improvement in the growth rate if exposed to excess glucose. The open circle trend refers to the growth rate trend observed when cells grown at D=0.37 were exposed to excess glucose. The open triangle trend refers to cells growing at their maximum growth rate on glucose. The open diamond trend refers to cells growing at D=0.34 exposed to excess glucose and excess amino acids. All data was scaled by their initial cell densities for trend comparison. [Reprinted without permission. **Harvey, R. J.** 1970. Metabolic regulation in glucose-limited chemostat cultures of Escherichia coli. J Bacteriol **104:**698-706. (Pages 669 and 702, Figures 1 and 6).]

Since amino acids are clearly a limiting factor in the growth rate of microbial cells the enzyme glutamate dehydrogenase (GDH) was thought to be a potential cause of the biosynthetic growth limitation. This enzyme is responsible for the majority of inorganic nitrogen assimilation in to cell biomass under carbon limited conditions and its amino acid product glutamate is required for the production of many other amino acids (26). For these reasons the enzyme was thought to be a better candidate for the intracellular growth limitation of microbial cells growing with substrate excess. To test this hypothesis cells precultured under glucose limited conditions were exposed to excess glucose and the cell density, RNA level, and GDH activity were all monitored during the transient. If the GDH enzyme was the cause of the intracellular limitation then the change in the enzyme's activity during transient conditions would mirror the change

seen in the RNA level as the production rate of ribosomes would be indirectly limited by the cell's production rate of glutamate.

5.2 Materials and Methods

5.2.1 Organism and Cultivation Conditions

The organism used in this work was *E. coli* ML308 (ATCC 15224) obtained from the American Type Culture collection. Cells were resuscitated from a frozen stock culture overnight on glucose (1 g/L) minimal media. The minimal media used in this work was described in the Materials and Methods Chapter and the components of which appear in Table 2-1. The chemostat cultures were grown in a 1.5 L Bioflow III fermenter (New Brunswick Scientific Co.) with a working volume of 1.2 L. The agitation speed was 1000 rpm and the aeration rate was 1.2 L/min. The bioreactor was equipped with automatic pH and temperature control. The pH was maintained at 7.0 $^{+}$/- 0.1 by addition of 1M KOH / 1M NaOH solution and 10% H_3PO_4 solutions. The temperature was maintained at 37^{o}C. The feed was pumped in by a Masterflex L/S peristaltic pump (7523-70) equipped with a Masterflex EZ Load pump head (7534-04). The reactor was equipped with a Vaisala GMT222 CO_2 analyzer for continuous monitoring of the carbon dioxide output of the reactor.

Chemostat cultures were precultured on glucose (200 mg/L) for four days at D=0.6 hr^{-1} before shifting to the trial dilution rate to ensure adaptation of the *E. coli* cells to low glucose conditions for reasons described in the Materials and Methods Chapter. The chemostat was then allowed to equilibrate for ten additional residence times to ensure the cells were adjusted to the new growth conditions (21). The cellular carbon dioxide evolution rate of the reactor was monitored during the adaptation and equilibration phases of preculturing to ensure the history and consequently the initial state of the chemostat grown cells were correct before attempting an experiment.

The cell density, RNA concentration, and GDH activity were measured by the methods covered in the Materials and Methods Chapter.

5.2.2 The Continuous to Batch Shift

Continuous to batch shifts with a subsequent glucose pulse were again employed to simulate the environment cells experience during a dilution rate shift up. The reactor media was pulsed with 1 g/L of glucose to ensure substrate level never became limiting during for length of the experiment. Towards the end of the experiment the cell density is rather high compared to the starting cell density and consequently the rate of substrate consumption would be high at this point as well. The duration of the experiment was decided to be two and a half hours long after finding an example GDH transient in the literature (18). The frequency of variable measurement and sample collection can be found in Table 5-1.

Table 5-1. Frequency of sample measurement / collection and approximate volume taken.

Sample	Vol. (mL)	Freq. (min)
Cell Density	6	5
RNA Level	2	10
GDH Activity	25	10

Note: Samples taken for GDH activity ranged from 5-25 mL depending on the cell density.

For qualitative comparison of the time evolution of all three variables the measured values were converted to a per liter of reactor volume basis and then scaled by their steady state value. The purpose of this analysis was to visualize the improvement in the ribosomal capacity and GDH biosynthetic capacity as it compared to the increase in cell density. Unfortunately the experiment was conducted only once at the intermediate dilution rate $D=0.3\ hr^{-1}$ due to time constraints.

5.3 Results and Discussion

The results of the measured trial conducted are displayed in Figure 5-3 and the scaled comparison of the three different variables appears in Figure 5-4. As hypothesized the scaled GDH activity level and RNA level of the reactor volume are qualitatively similar initially upon exposure of the culture to excess glucose. This data coupled with the fact that amino acids instantly increase the growth rate of *E. coli* beyond the maximum attainable growth rate supports the idea that GDH and not ribosome level is the better candidate for the biosynthetic growth limitation. Unfortunately one trial at one preculture dilution rate is not sufficient to make this a substantial conclusion.

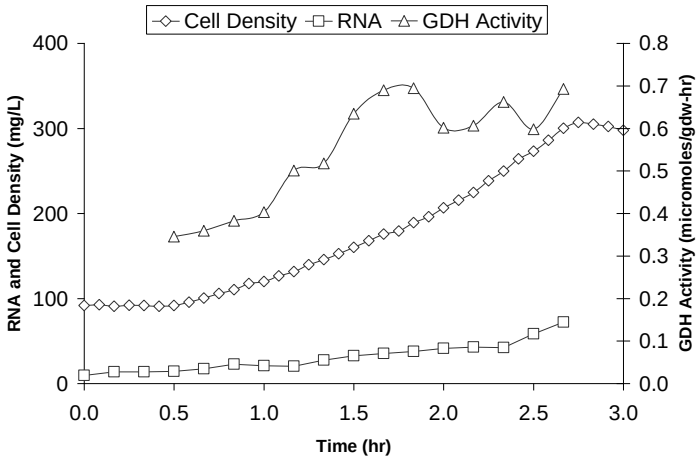

Figure 5-3. Data obtained from a continuous to batch shift of glucose limited *E. coli* ML308 precultured at D=0.3 hr^{-1} to excess glucose. The feed concentration of glucose was 200 mg/L and the glucose pulse at half an hour was to 1 g/L glucose.

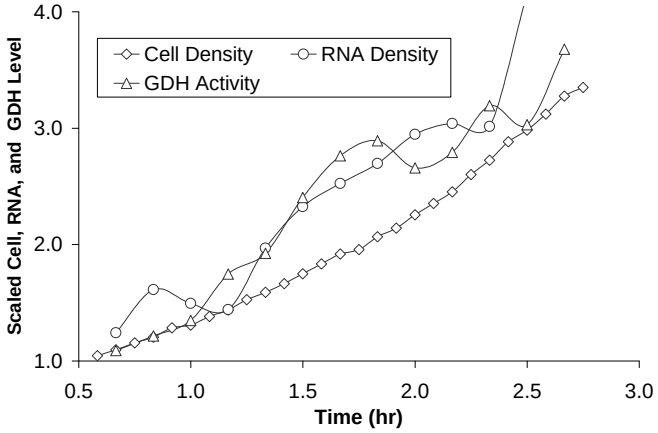

Figure 5-4. Data from Figure 5-3 converted to a per liter basis and scaled by their steady state value for the purpose of trend comparison.

Another interesting discovery was found when trying to find a way to analyze the data from this experiment was the presence of major oscillations in the growth rate with time upon exposure of carbon limited microbial cells to excess carbon. Fifteen minute growth rate fits were calculated for each cell density measurement collected using the cell density measurements five minutes before and five minutes after. The seemingly large amount of scatter seen in the collected data was first attributed to spectrometer noise, operator error, or a mechanical forcing influence brought about by the reactor itself. All three of these sources of oscillation were eliminated by a simple shake flask experiment where nothing but the cell density was measured. The magnitude and time interval of the oscillations from the reactor trial and the shake flask trial were similar. The properties of the mechanical shaker were much different then those of the reactor setup supporting the idea that the observed oscillations were a cell driven phenomenon. The results of the reactor and shake flask growth rate trials appear in Figure 5-5. The cause of these oscillations is still an unknown up to this point.

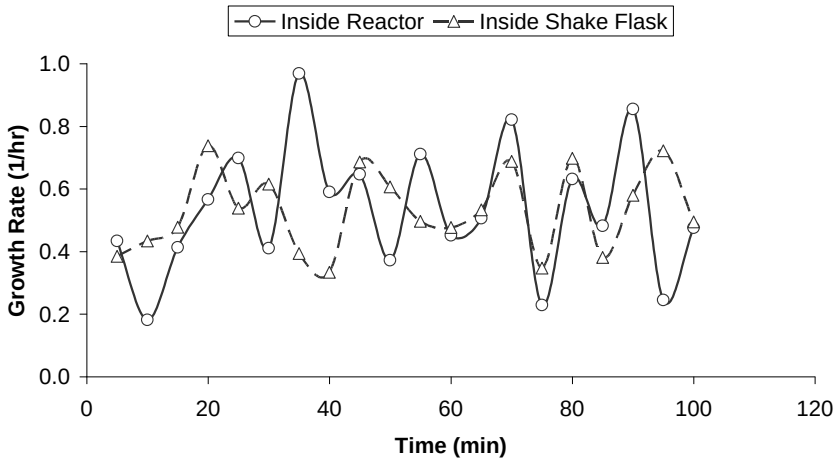

Figure 5-5. Oscillations present in growth rate of glucose limited cells exposed to excess glucose. Cells were precultured at D=0.3 hr^{-1} on 200 mg/L glucose minimal media. Upon extraction or a switch to batch mode the reactor volume was pulsed with glucose to a concentration of 1 g/L. The experiment was done in a shake flask as well as in a reactor to ensure mechanical oscillations were not forcing the cell growth rate oscillations.

CHAPTER 6
CONCLUDING REMARKS

The study was a success from the point of view that new knowledge is available for understanding how microorganisms respond to the environment around them. Even the time spent on protocol validation and system characterization provided information on *E. coli* not published in the literature: protein and RNA content versus glucose limited dilution rate and low dilution rate growth response of glucose limited cells exposed to excess glucose. The experiments completed provide further insight in to how microorganisms respond to removal of the nutrient growth limitation.

The carbon flux experiments provided a lot of insight in to how the cell utilizes substrate before and after exposure to excess glucose at different glucose limited growth rates. Cells grown at all dilution rates tested were able to instantly improve their growth rate and substrate uptake rate upon removal of the glucose growth limitation. How the cells utilize this excess glucose is highly dependent on the preculture glucose limited growth rate.

Unfortunately the biosynthetic limitation experiments remain incomplete due to time constraints but it still remains that ribosomes are not the key cause of biosynthetic limitation as excess amino acids will greatly speed the growth rate of carbon limited microbial cells. The data that was collected did support the hypothesis that the enzyme glutamate dehydrogenase mirrors the RNA concentration well and could be the cause of biosynthetic limitation rather then the ribosome level. The detection of oscillations in growth rate of glucose limited cells exposed to excess glucose was not the purpose of the experiments here but was found regardless. This is a prime example of how research can answer questions but in the end can pose more. Finding the source of this specific growth rate oscillation would be the potential next step in this research.

APPENDIX A
VISUAL BASIC PROGRAM FOR THE VAISALA GMT222 CO2 ANALYZER

CODE

```
Public CO2, X As Single
Public CollectingData As Boolean
Dim CO2Array(1 To 720, 1 To 2) As Single
Public ClockSeconds, ClockMinutes, ClockHours, TotalCollectionTime, MinuteTimer As Integer

Sub GetCO2()
‘Queries the detector for a value and rounds the value to the nearest ppm
CO2 = MSComm1.Input
CO2 = Round(Val(CO2), 0)
End Sub

Private Sub Form_Load()
'Initialization subroutine. Setup for COM Port, array for data storage, and main chart.
MSComm1.InBufferSize = 6
MSComm1.CommPort = 6
MSComm1.PortOpen = True

For X = 0 To 39
   RealTime.List(X) = ""
Next X
For X = 1 To 720
      CO2Array(X, 1) = X
      CO2Array(X, 2) = 0
Next X
With CO2Chart
   .chartType = VtChChartType2dXY
   .Plot.UniformAxis = False
   .Plot.SeriesCollection(1).ShowLine = False
   .Plot.SeriesCollection(1).SeriesMarker.Auto = False
   .Plot.SeriesCollection(1).DataPoints(-1).Marker.Style = VtMarkerStyleFilledCircle
   .Plot.SeriesCollection(1).DataPoints(-1).Marker.Size = 60
   .Plot.SeriesCollection(1).DataPoints(-1).Marker.Visible = True
   .Plot.AutoLayout = False
   .Plot.Axis(VtChAxisIdY).ValueScale.Auto = False
   .Plot.Axis(VtChAxisIdY).ValueScale.Maximum = 1000
   .Plot.Axis(VtChAxisIdY).ValueScale.Minimum = 0
   .Plot.Axis(VtChAxisIdY).ValueScale.MajorDivision = 10
   .Plot.Axis(VtChAxisIdX).ValueScale.Auto = False
   .Plot.Axis(VtChAxisIdX).ValueScale.Maximum = 720
   .Plot.Axis(VtChAxisIdX).ValueScale.Minimum = 0
```

```
    .Plot.Axis(VtChAxisIdX).ValueScale.MajorDivision = 12
    .Plot.Axis(VtChAxisIdY).AxisTitle = "CO2 Concentration (ppm)"
    .Plot.Axis(VtChAxisIdX).AxisTitle = "Data Point Taken Every Minute"
    .ChartData = CO2Array
End With
End Sub


Private Sub Updategraph()
‘Updates the data array and adjusts  the chart accordingly.
If MinuteTimer = 60 Then MinuteTimer = 0
MinuteTimer = MinuteTimer + 1
If MinuteTimer Mod 60 = 0 Then
    For X = 1 To 719
        CO2Array(721 - X, 2) = CO2Array(720 - X, 2)
    Next X
    CO2Array(1, 2) = CO2
    CO2Chart.ChartData = CO2Array
End If
End Sub

Private Sub SendCommandButton_Click()
‘Sends text input directly to the Vaisala GMT222 CO2 Analyzer
MSComm1.Output = Command.Text
End Sub

Private Sub StartCollectionButton_Click()
‘Starts a text file with the entered name and starts recording timestamped data to the file.
‘Also starts the data collection clock.
If Interval.Text = "" Or Filename.Text = "" Then
Else
    Open Filename.Text For Output As #1
    Print #1, "Time (sec),CO2 (ppm)"
    CollectingData = True
    Interval.Locked = True
    Filename.Locked = True
    StartCollectionButton.Enabled = False
    SendCommandButton.Enabled = False
End If
End Sub

Private Sub StopCollectionButton_Click()
‘Stop recording to the data file and shuts the data collection clock off.
Close #1
CollectingData = False
Interval.Locked = False
```

```
Filename.Locked = False
StartCollectionButton.Enabled = True
SendCommandButton.Enabled = True
Hours.Caption = 0
Minutes.Caption = 0
Seconds.Caption = 0
End Sub

Private Sub Timer1_Timer()
‘Subroutines called every time interval to collect data and update the chart.
Call RealTimeCO2
Call DataCollectionClock
Call Updategraph
Call DataCollection
End Sub

Private Sub RealTimeCO2()
‘Updates the real time CO2 to the left of the chart. Values shown every second.
Call GetCO2
For X = 0 To 39
   RealTime.List(39 - X) = RealTime.List(38 - X)
Next X
RealTime.List(0) = CO2
End Sub

Private Sub DataCollectionClock()
‘Subroutine for the Data Collection Clock seen to the right of the chart.
If CollectingData = True Then
   ClockHours = Val(Hours.Caption)
   ClockMinutes = Val(Minutes.Caption)
   ClockSeconds = Val(Seconds.Caption)
   ClockSeconds = ClockSeconds + 1
   If ClockSeconds = 60 Then
      ClockMinutes = ClockMinutes + 1
      ClockSeconds = 0
   End If
   If ClockMinutes = 60 Then
      ClockHours = ClockHours + 1
      ClockMinutes = 0
   End If
   Hours.Caption = ClockHours
   Minutes.Caption = ClockMinutes
   Seconds.Caption = ClockSeconds
   TotalCollectionTime = ClockHours * 3600 + ClockMinutes * 60 + ClockSeconds
End If
End Sub
```

```
Private Sub DataCollection()
'Subroutine that prints the current value to the data file if data recording is active.
If CollectingData = True Then
   If TotalCollectionTime Mod Val(Interval.Text) = 0 Then
      Print #1, Str(TotalCollectionTime) + "," + Str(CO2)
   End If
End If
End Sub
```

FORM SETUP

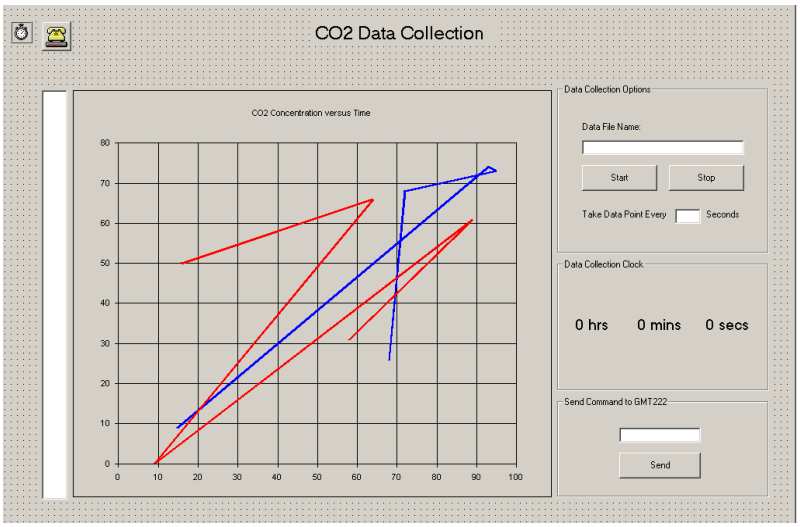

USER INTERFACE

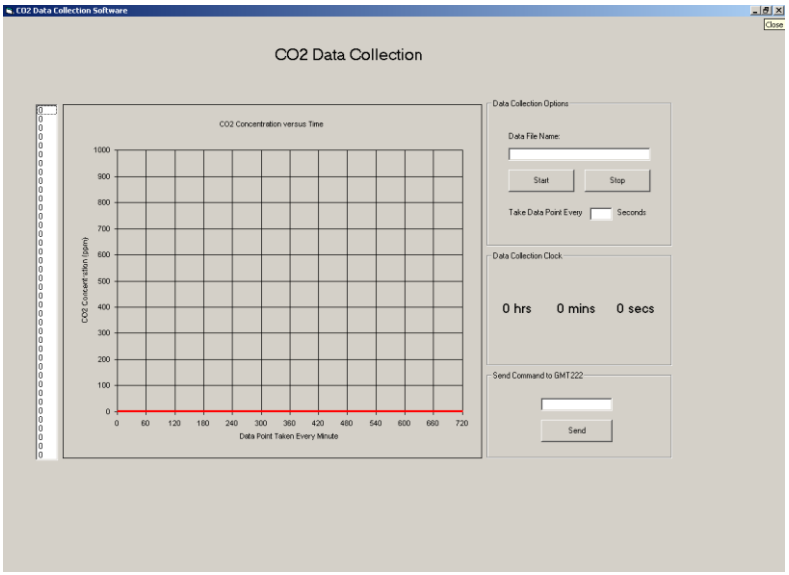

APPENDIX B
RESULTS OF CARLO ERBA-1106 ELEMENTAL ANALYSIS OF E. COLI ML308

Elemental Analysis Done on the Carlo Erba-1106 Elemental Analyzer

D (1/hr)	N (g/gdw)	C (g/gdw)	H (g/gdw)
0.1	0.12	0.46	0.07
	0.11	0.43	0.07
	0.11	0.43	0.07
	0.11	0.43	0.07
	0.11	0.43	0.07
0.2	0.12	0.46	0.07
	0.11	0.42	0.07
	0.11	0.42	0.07
	0.12	0.47	0.07
	0.12	0.47	0.07
0.3	0.12	0.46	0.07
	0.12	0.46	0.07
	0.12	0.45	0.07
	0.12	0.45	0.07
	0.12	0.45	0.07
0.4	0.12	0.46	0.07
	0.11	0.43	0.07
	0.11	0.43	0.07
	0.12	0.45	0.07
	0.12	0.45	0.07
0.5	0.12	0.46	0.07
	0.11	0.39	0.07
	0.11	0.38	0.07
	0.12	0.45	0.07
	0.12	0.45	0.07
0.6	0.11	0.39	0.07
	0.11	0.39	0.07
	0.12	0.41	0.07
	0.11	0.41	0.07
	0.12	0.44	0.07
	0.12	0.43	0.07

Elemental Analysis Statistics

D (1/hr)	Ave N	Ave C	Ave H	StDev N	StDev C	StDev H	RSD N	RSD C	RSD H
0.1	0.11	0.44	0.07	0.01	0.01	0.00	0.06	0.03	0.03
0.2	0.12	0.45	0.07	0.01	0.02	0.00	0.05	0.05	0.01
0.3	0.12	0.46	0.07	0.00	0.00	0.00	0.02	0.01	0.01
0.4	0.12	0.44	0.07	0.00	0.01	0.00	0.04	0.03	0.02
0.5	0.12	0.43	0.07	0.01	0.04	0.00	0.06	0.08	0.03
0.6	0.12	0.41	0.07	0.01	0.02	0.00	0.05	0.05	0.02

LIST OF REFERENCES

1. **Aiba, S., N. Y. Nishizawa, and M. Onodera.** 1967. Nucleic approach to some response of chemostatic culture of Azobacter vinelandii. Gen. Appl. Microbiol. **35:**85-101.

2. **Bally, M., and T. Egli.** 1996. Dynamics of Substrate Consumption and Enzyme Synthesis in Chelatobacter heintzii during Growth in Carbon-Limited Continuous Culture with Different Mixtures of Glucose and Nitrilotriacetate. Appl Environ Microbiol **62:**133-140.

3. **Benov, L., and J. Al-Ibraheem.** 2002. Disrupting Escherichia coli: a comparison of methods. J Biochem Mol Biol **35:**428-31.

4. **Benthin, S., and J. Villadsen.** 1991. Growth energetics of Lactococcus cermoris FD1 during energy-carbon and nitrogen limitation in steady state and transient cultures. Chem. Eng. Sc. **49:**589-609.

5. **Brunschede, H., T. L. Dove, and H. Bremer.** 1975. Establishment of exponential growth after a nutritional shift-up in Escherichia coli B/r: Accumulation of deoxyribonucleic acid, ribonucleic acid, and protein. J Bacteriol **129:**1020-1033.

6. **Brunschede, H., T. L. Dove, and H. Bremer.** 1975. Establishment of exponential growth after a nutritional shift-up in Escherichia coli B/r: Accumulation of deoxyribonucleic acid, ribonucleic acid, and protein. J Bacteriol **129:**355-358.

7. **Cataldi, T. R., C. Campa, M. Angelotti, and S. A. Bufo.** 1999. Isocratic separations of closely-related mono- and disaccharides by high-performance anion-exchange chromatography with pulsed amperometric detection using dilute alkaline spiked with barium acetate. J Chromatogr A **855:**539-50.

8. **Cataldi, T. R. I., C. Campa, and G. E. De Benedetto.** 2000. Carbohydrate analysis by high-performance anion-exchange chromatography with pulsed amperometric detection: The potential is still growing. Fresenius Journal of Analytical Chemistry **368:**739-758.

9. **Chi, C. T., and J. A. Howell.** 1976. Transient behavior of a continuous stirred tank biological reactor utilizing phenol as an inhibitory substrate. Biotechnol Bioeng **18:**63-80.

10. **Cooney, C. L., and D. I. Wang.** 1976. Transient response of Enterobacter aerogenes under a dual nutrient limitation in a chemostat. Biotechnol Bioeng **18:**189-98.

11. **Cooney, C. L., D. I. Wang, and R. I. Mateles.** 1976. Growth of Enterobacter aerogenes in a chemostat with double nutrient limitations. Appl Environ Microbiol **31:**91-8.

12. **Daniels, L., R. S. Hanson, and J. A. Phillips.** 1994. Chemical Analysis. American Society of Microbiology.

13. **Duboc, P., U. von Stockar, and J. Villadsen.** 1998. Simple generic model for dynamic experiments with Saccharomyces cerevisiae in continuous culture: decoupling between anabolism and catabolism. Biotechnol Bioeng **60:**180-9.

14. **EH&S.** 1998. Biological Safety Manual. University of Florida, Gainesville, FL.

15. **Gerhardt, P., R. G. E. Murray, W. A. Wood, and N. R. Krieg.** 1994. Methods for General and Molecular Bacteriology. American Society of Microbiology, Washington, D. C.

16. **Han, K., H. C. Lim, and J. Hong.** 1992. Acetic-Acid Formation in Escherichia-Coli Fermentation. Biotechnology and Bioengineering **39:**663-671.

17. **Hans-Peter Meyer, e. a.** 1984. Acetate formation in continuous culture of E. coli K12 D1 on defined and complex media. Journal of Biotechnology **1:**355-358.

18. **Harvey, R. J.** 1970. Metabolic regulation in glucose-limited chemostat cultures of Escherichia coli. J Bacteriol **104:**698-706.

19. **Herbert, D., R. Elsworth, and R. C. Telling.** 1956. The continuous culture of bacteria; a theoretical and experimental study. J Gen Microbiol **14:**601-22.

20. **Koch, A. L., and C. S. Deppe.** 1971. In vivo assay of protein synthesizing capacity of Escherichia coli from slowly growing chemostat cultures. J Mol Biol **55:**549-62.

21. **Lendenmann, U.** 1994. Growth Kinetics of Escherichia coli with mixtures of sugars.

22. **Lendenmann, U., and T. Egli.** 1995. Is Escherichia coli growing in glucose-limited chemostat culture able to utilize other sugars without lag? Microbiology **141 (Pt 1):**71-8.

23. **Lin, R. I. S., and O. A. Schjeide.** 1969. Micro Estimation of Rna by Cupric Ion Catalyzed Orcinol Reaction. Analytical Biochemistry **27:**473-&.

24. **Maaloe, O. a. N. O. K.** 1966. A study of DNA, RNA, and protein synthesis. W. A. Benjamin, New York.

25. **Maier, R. M., I. L. Pepper, and C. P. Gerba.** 2000. Envrionmental Microbiology. Academic Press, San Diego, CA.

26. **Meers, J. L., D. W. Tempest, and C. M. Brown.** 1970. 'Glutamine(amide):2-oxoglutarate amino transferase oxido-reductase (NADP); an enzyme involved in the synthesis of glutamate by some bacteria. J Gen Microbiol **64:**187-94.

27. **Nagai, S., Y., Nishizawa, I. Endo, and S. Aiba.** 1968. Response of a chemostatic culture of Azobacter vinelandii to a delta type pulse of glucose. J. Gen. Appl. Microbiol. **14:**121-134.

28. **Natarajan, A., and F. Srienc.** 2000. Glucose uptake rates of single E. coli cells grown in glucose-limited chemostat cultures. J Microbiol Methods **42:**87-96.

29. **Neidhardt, F. C. e. a.** 1990. Physiology of the Bacterial Cell: A Molecular Approach. Frank Sinauer Associates, Sunderland.

30. **Neijssel, M., S. Hueting, and D. W. Tempest.** 1977. Glucose transport capacity is not rate-limiting in the growth of some wild-type strains of Escherichia coli and Klebsiella aerogen in chemostat culture. FEMS Microbiol Lett **2:**1-3.

31. **Nielsen, J., and J. Villadsen.** 1992. Modelling of Microbial Kinetics. Chem. Eng. Sc. **47:**4225-4270.

32. **Obrien, R. W., O. M. Neijssel, and D. W. Tempest.** 1980. Glucose Phosphoenolpyruvate Phosphotransferase Activity and Glucose-Uptake Rate of Klebsiella-Aerogenes Growing in Chemostat Culture. Journal of General Microbiology **116:**305-314.

33. **Phipps, D. W. T. a. P. J.** 1967. Studies on the growth of Aerobacter aerogenes at low dilution rates in a chemostat. Microbial Physiology and Continuous Culture. Her Majesty's Stationary Office**:**240-253.

34. **Pierce Biotechnology, I.** 2003. BCA Protein Assay Kit, Rockford, IL.

35. **Primrose, S. B., and A. C. Wardlaw.** 1982. Sourcebook of Experiments for the Teaching of Microbiology. Academic Press, St. Louis, MO.

36. **Ramkrishna, B. a.** 1990. Metabolic regulation in bacterial continuous cultures. Biotechnol Bioeng **29:**940-943.

37. **Schulze, U., M. E. Larsen, and J. Villadsen.** 1995. Determination of intracellular trehalose and glycogen in Saccharomyces cerevisiae. Anal Biochem **228:**143-9.

38. **Schwinghamer, E. A.** 1980. Method for Improved Lysis of Some Gram-Negative Bacteria. Fems Microbiology Letters **7:**157-162.

39. **Scopes, R. K.** 1994. Protein Purification, 3rd ed. Springer+Business Media, Inc., New York, NY.

40. **Senior, P. J.** 1975. Regulation of nitrogen metabolism in Escherichia coli and Klebsiella aerogenes: studies with the continuous-culture technique. J Bacteriol **123:**407-18.

41. **Senn, H., U. Lendenmann, M. Snozzi, G. Hamer, and T. Egli.** 1994. The growth of Escherichia coli in glucose-limited chemostat cultures: a re-examination of the kinetics. Biochim Biophys Acta **1201:**424-36.

42. **Sonnleitner, B., S. A. Rothen, and H. Kuriyama.** 1997. Dynamics of glucose consumption in yeast. Biotechnol Prog **13:**8-13.

43. **Standing, C. N., A. G. Fredrickson, and H. M. Tsuchiya.** 1972. Batch- and continuous-culture transients for two substrate systems. Appl Microbiol **23:**354-9.

44. **Teplitksi, M.** 2007. Method for Bead Disruption of Starved Microorganisms. *In* J. Noel (ed.), Gainesville, FL.

45. **Wick, L. M., M. Quadroni, and T. Egli.** 2001. Short- and long-term changes in proteome composition and kinetic properties in a culture of Escherichia coli during transition from glucose-excess to glucose-limited growth conditions in continuous culture and vice versa. Environ Microbiol **3:**588-99.

46. **Yagil, G., and E. Yagil.** 1971. Relation between Effector Concentration and Rate of Induced Enzyme Synthesis. Biophysical Journal **11:**11-&.

47. **Yang, S. S., M. Miller, J. Martin, and J. Harris.** 2003. Evaluation and Application of a New Total Organic Carbon Analyzer, Teledyne Instruments Application Note, Mason, OH.

48. **Yun, H. S., J. Hong, and H. C. Lim.** 1996. Regulation of ribosome synthesis in Escherichia coli: Effects of temperature and dilution rate changes. Biotechnology and Bioengineering **52:**615-624.

BIOGRAPHICAL SKETCH

Jason Noel received his B.S. from Virginia Commonwealth University in Richmond, Virginia in August of 2003. Thereafter he has worked as a graduate student in the Chemical Engineering Department of the University of Florida studying the growth kinetics of bacteria and received his doctorial degree in August of 2007.